



中国科学院
CHINESE ACADEMY OF SCIENCES



Institute of Modern Physics, Chinese Academy of sciences

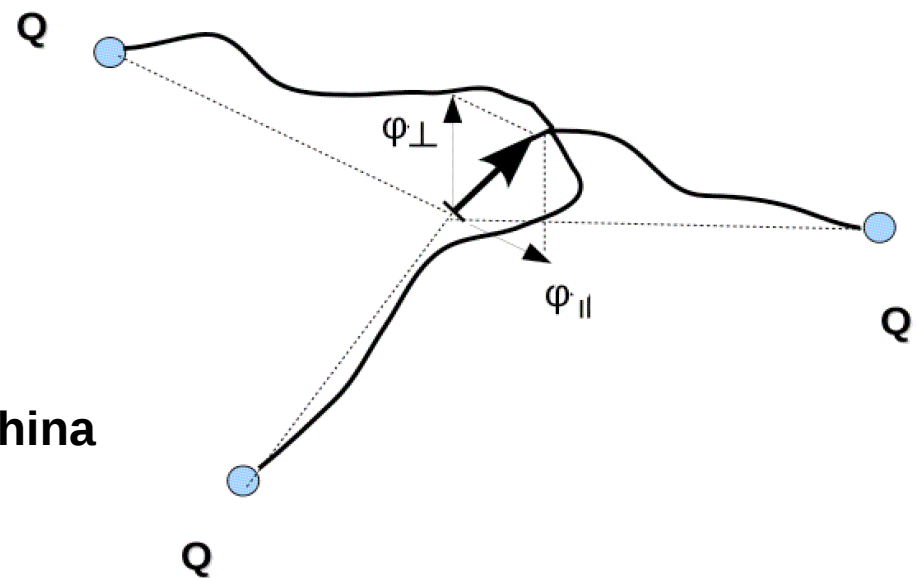
The Confining Y-Baryonic Strings on the Lattice

Presenter: Ahmed Bakry

**Collaborators:
Xurong Chen,
Pengming Zhang**

Institute of Modern Physics, Lanzhou, China

**Confinement XI
Saint Petersburg - Russia**



Talk summary

- Motivation
- Lattice Measurements
- Baryonic String model
- Results

Motivation

- The string picture's main measurable universal consequences of the Luscher subleading correction to the QQ potential and flux-tube logarithmic growth law have been verified with the lattice data at large distances.
- The study of the stringlike behaviour of flux tubes in multi-quark systems is less visited on the lattice due to the practical difficulty of the noisy signal.
- There have been difficulties to unravel an unbiased form of the action density distribution. This has presented hitherto a challenge to directly scrutinize the baryonic strings on the lattice unambiguously.
- The action density correlation with three Polyakov loops has displayed a filled Δ -shaped profile. This filled Δ -shaped arrangement surprisingly persists to large inter-quark separations.
- A look at the signatures of the baryonic strings in lattice data is an interesting topic for quark confinement that has not been yet addressed in SU(3) pure gauge theory.

Lattice Measurements: Flux correlation function

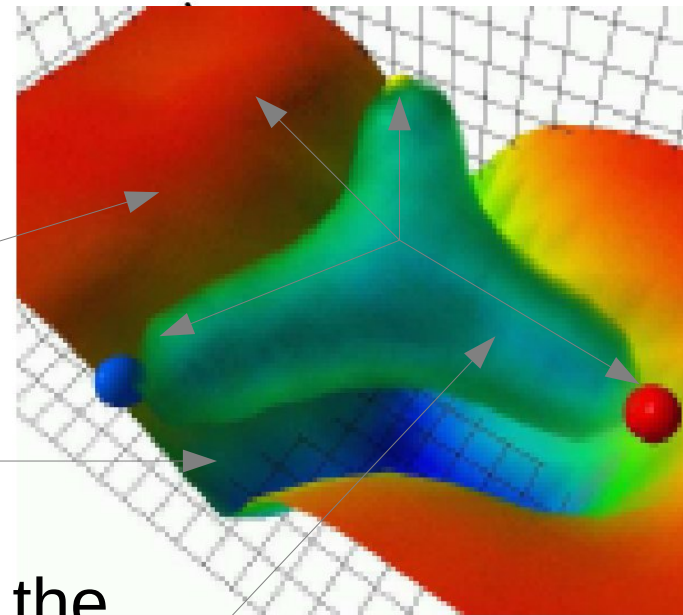
The form of the correlation function for the action density,

$$C(\vec{y}, \vec{r}_1, \vec{r}_2, \vec{r}_3, \tau) = \frac{\langle W_{3Q}(\vec{r}_1, \vec{r}_2, \vec{r}_3; \tau) S(\vec{y}, \tau/2) \rangle}{\langle W_{3Q}(\vec{r}_1, \vec{r}_2, \vec{r}_3; \tau) \rangle \langle S(\vec{y}, \tau/2) \rangle} \quad (1)$$

C is a scalar field in three dim.

$$C = 1$$

$$C < 1$$


$$\vec{r}_i$$

$C < 1$, signaling the expulsion of the vacuum fluctuation from the interior of the baryonic system.

Flux correlation function

Constructing the baryon by Wilson 3Q operator

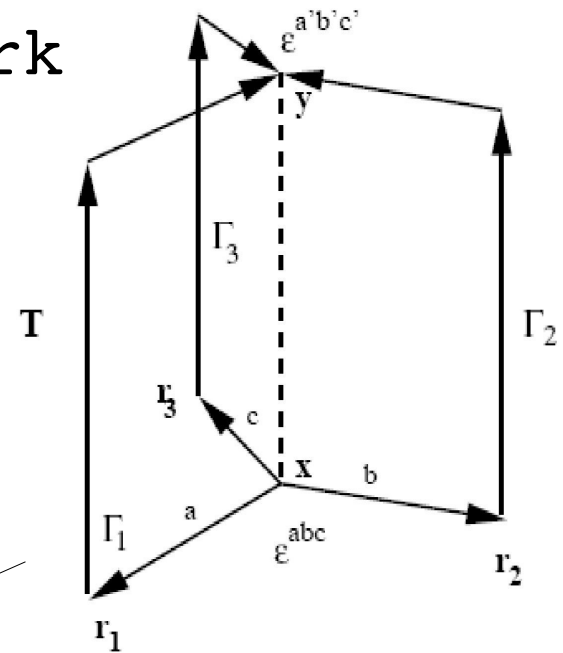
The generic form of the three-quark Wilson loop is given by,

$$W_{3Q} = \frac{1}{3!} \varepsilon_{abc} \varepsilon_{a'b'c'} U_1^{aa'} U_2^{bb'} U_3^{cc'}$$

With the path-ordered link variables,

$$U_j = P \exp \left\{ ig \int_{\Gamma_j} dx_\mu A^\mu(x) \right\}$$

$$C(\vec{y}, \vec{r}_1, \vec{r}_2, \vec{r}_3, \tau) = \frac{\langle W_{3Q}(\vec{r}_1, \vec{r}_2, \vec{r}_3; \tau) S(\vec{y}, \tau/2) \rangle}{\langle W_{3Q}(\vec{r}_1, \vec{r}_2, \vec{r}_3; \tau) \rangle \langle S(\vec{y}, \tau/2) \rangle}$$

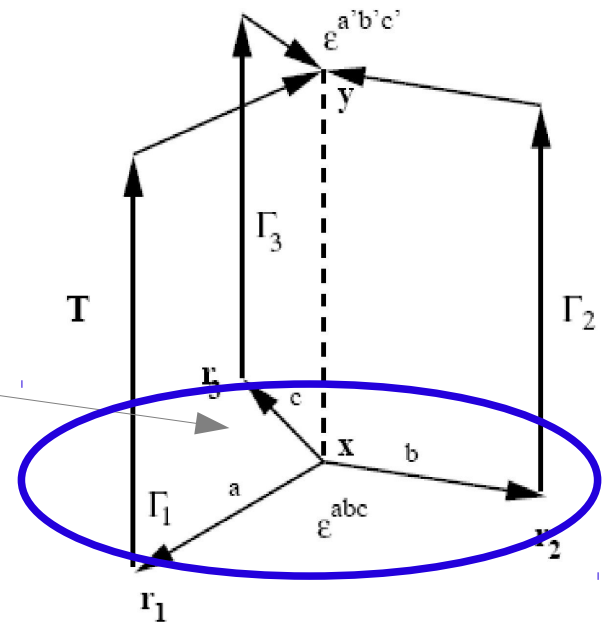
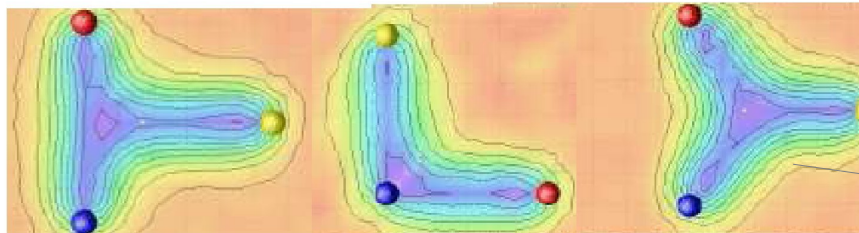


(1)

Biasing by the quark source operator

For a fixed source geometry, many different string configurations are possible.

Dependence on the choice of the source operator indicates that non-ground state contaminations contribute to the correlation function .



Difficulty in isolating the ground state

$$C(\vec{y}, \vec{r}_1, \vec{r}_2, \vec{r}_3, \tau) = \frac{\langle W_{3Q}(\vec{r}_1, \vec{r}_2, \vec{r}_3; \tau) S(\vec{y}, \tau/2) \rangle}{\langle W_{3Q}(\vec{r}_1, \vec{r}_2, \vec{r}_3; \tau) \rangle \langle S(\vec{y}, \tau/2) \rangle} \quad (1)$$

The two-point correlation function,

$$\begin{aligned} \langle \Omega | O(T) O(0) | \Omega \rangle &= \sum_n e^{-E_n T} \langle \Omega | O(0) | n \rangle \langle n | O(0) | \Omega \rangle \\ &\longrightarrow e^{-E_0 T} \langle \Omega | O(0) | 0 \rangle \langle 0 | O(0) | \Omega \rangle \end{aligned}$$

The three-point correlation function,

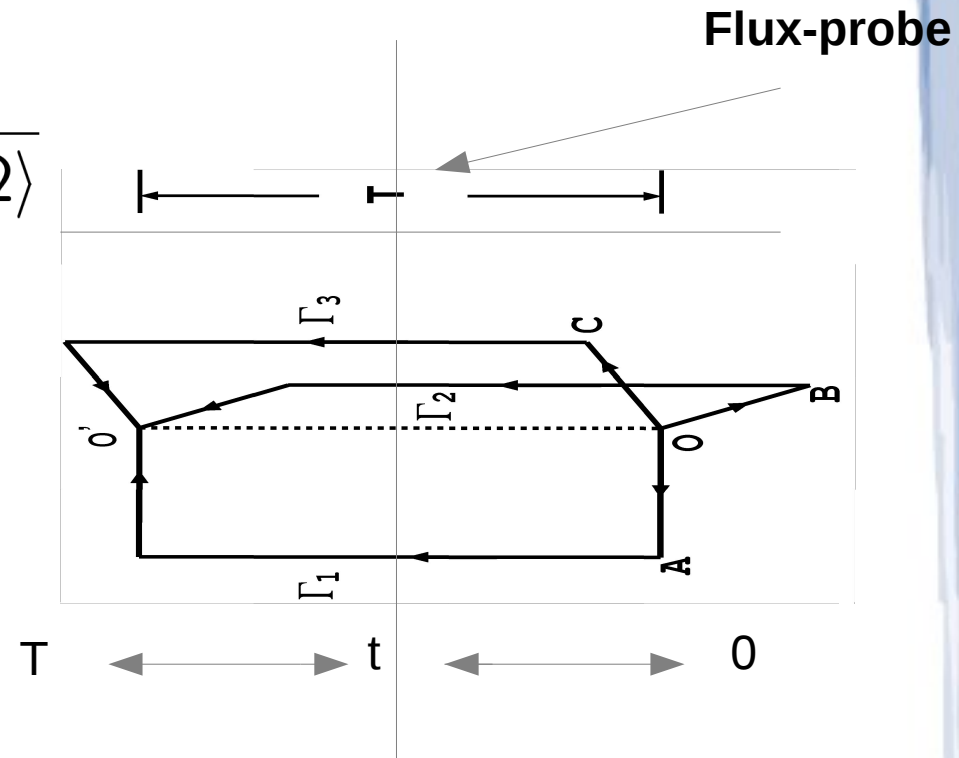
$$\begin{aligned} \langle \Omega | O(T) P(t) O(0) | \Omega \rangle &= \sum_{nn'} e^{-E_n(T-t)} e^{-E_{n'} t} \\ &\quad \times \langle \Omega | O(0) | n \rangle \langle n | P(0) | n' \rangle \langle n' | O(0) | \Omega \rangle \\ &\rightarrow e^{-E_0 T} \langle \Omega | O(0) | 0 \rangle \langle 0 | P(0) | 0 \rangle \langle 0 | O(0) | \Omega \rangle \end{aligned}$$

The correlation function which gives the field distribution is then,

$$C(t) = \frac{\langle \Omega | O(T) P(t) O(0) | \Omega \rangle}{\langle \Omega | O(T) O(0) | \Omega \rangle \langle \Omega | P(0) | \Omega \rangle}$$

$$\rightarrow \frac{\langle 0 | P(0) | 0 \rangle}{\langle \Omega | P(0) | \Omega \rangle}$$

$$0 \ll t \ll T$$



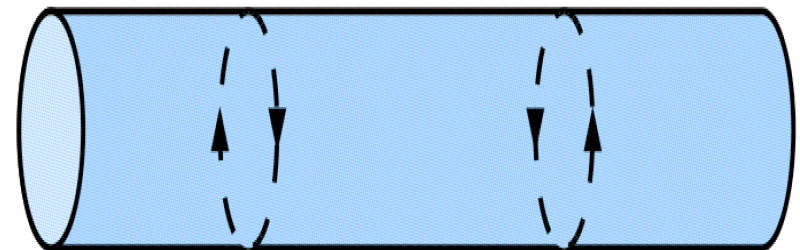
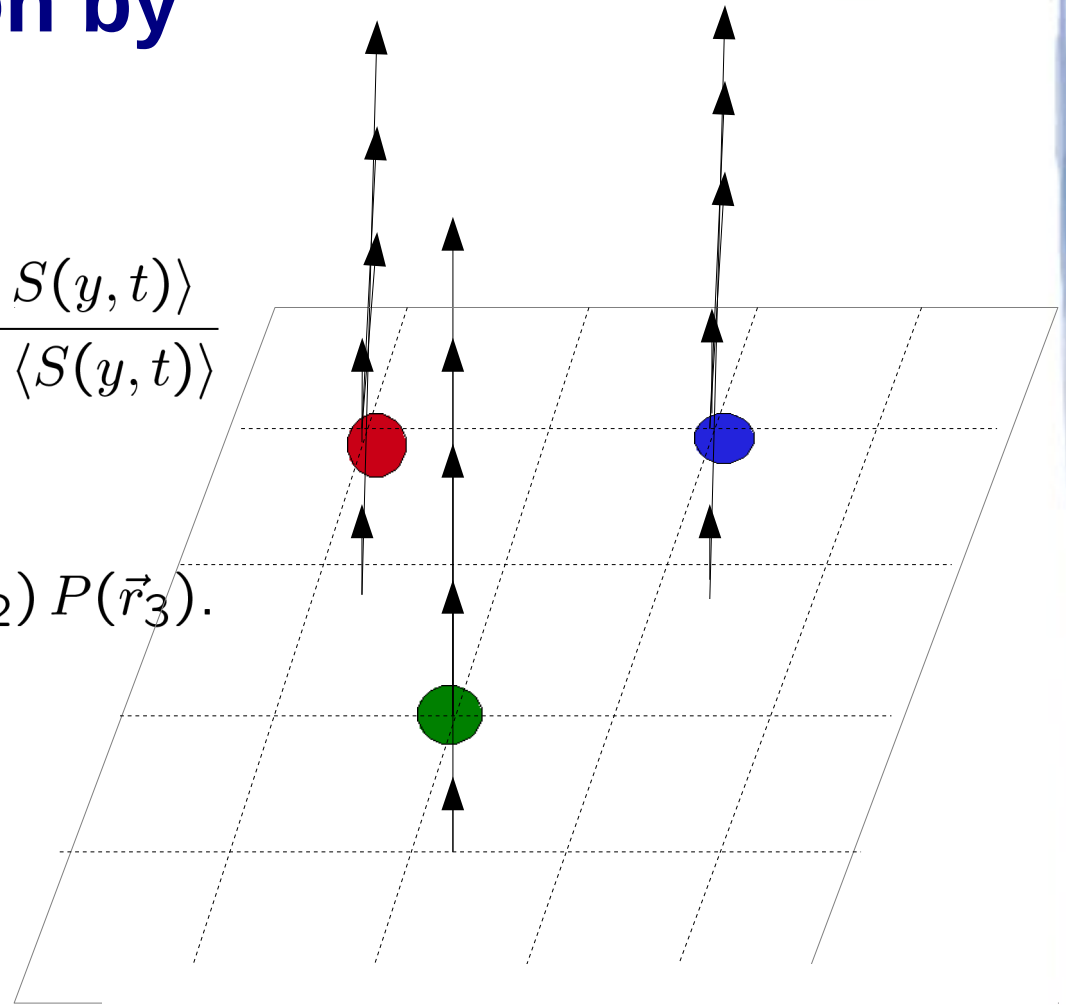
The correlation function is a measure of the ground state expectation value of the operator to that of the vacuum.

Biasing by the shape of the source strings must mean that non-ground state contaminations contribute to the correlation function .

Constructing the baryon by three-Polyakov loops

$$C(\vec{y}, \vec{r}_1, \vec{r}_2, \vec{r}_3) = \frac{\langle \mathcal{P}_{3Q}(\vec{r}_1, \vec{r}_2, \vec{r}_3) S(y, t) \rangle}{\langle \mathcal{P}_{3Q}(\vec{r}_1, \vec{r}_2, \vec{r}_3) \rangle \langle S(y, t) \rangle}$$

where $\mathcal{P}_{3Q}(\vec{r}_1, \vec{r}_2, \vec{r}_3) = P(\vec{r}_1) P(\vec{r}_2) P(\vec{r}_3)$.



$Y=ma$

$X=na$

Method (Noise Reduction).

A- Stout-Link smearing.

B- Lattice symmetries.

C- Monte-Carlo Updates.

D- Quark configuration symmetries.

Simulation set up

The gauge configurations were generated using the standard Wilson gauge action. The two lattices employed in this investigations are being of a typical spatial size of $N_s=36 \times 36 \times 36, N_t=10$, $N_s=36 \times 36 \times 36, N_t=8$.

Performing the simulations on large enough lattice sizes would be beneficial to gain high statistics in a gauge-independent manner and also minimizing the mirror effects and correlations across the boundaries as a by-product.

The SU(3) gluonic gauge configurations has been generated employing a pseudo-heatbath algorithm “Fabricius,Kennedy” updating the corresponding three SU(2) subgroup elements.

Each update step consists of one heat bath and 5 micro-canonical reflections. We choose to perform our analysis with lattices as fine as $a = 0.1$ fm by adopting a coupling of value $\beta = 6.00$, with temporal extents of $N_t = 8$, and $N_t = 10$ slices, which correspond to temperatures $T = 0.8, 0.9 T_c$,

We perform a set of measurements $n=20$ separated by 70 sweeps of updates. Each set of measurements is taken following a 2000 of updating sweeps. These sub-measurements are binned together in evaluating. The total measurements taken on 500 bins.

In this investigation, we have taken 10,000 measurement at each temperature. The measurements are taken on hierarchically generated configurations.

Simulation set up

The gauge configurations were generated using the standard Wilson gauge action. The two lattices employed in this investigations are being of a typical spatial size of $N_s=36 \times 36 \times 36, N_t=10$, $N_s=36 \times 36 \times 36, N_t=8$.

Performing the simulations on large enough lattice sizes would be beneficial to gain high statistics in a gauge-independent manner and also minimizing the mirror effects and correlations across the boundaries as a by-product.

The SU(3) gluonic gauge configurations has been generated employing a pseudo-heatbath algorithm “Fabricius,Kennedy” updating the corresponding three SU(2) subgroup elements.

Each update step consists of one heat bath and 5 micro-canonical reflections. We choose to perform our analysis with lattices as fine as $a = 0.1$ fm by adopting a coupling of value $\beta = 6.00$, with temporal extents of $N_t = 8$, and $N_t = 10$ slices, which correspond to temperatures $T = 0.8, 0.9 T_c$,

We perform a set of measurements $n=20$ separated by 70 sweeps of updates. Each set of measurements is taken following a 2000 of updating sweeps. These sub-measurements are binned together in evaluating. The total measurements taken on 500 bins.

In this investigation, we have taken 10,000 measurement at each temperature. The measurements are taken on hierarchically generated configurations.

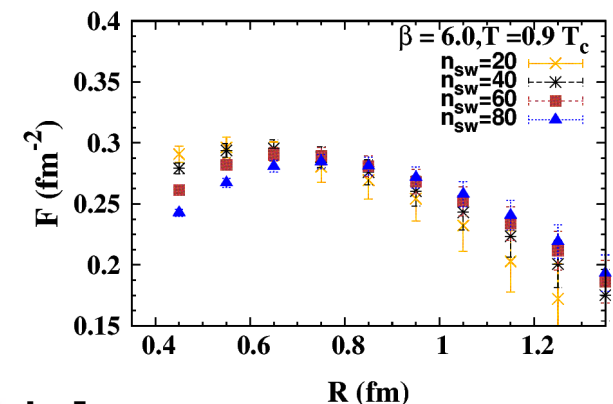
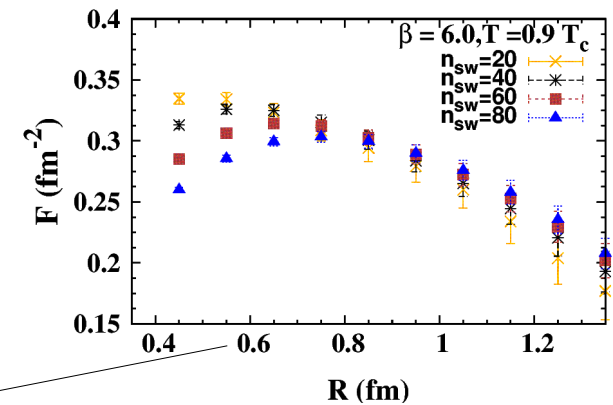
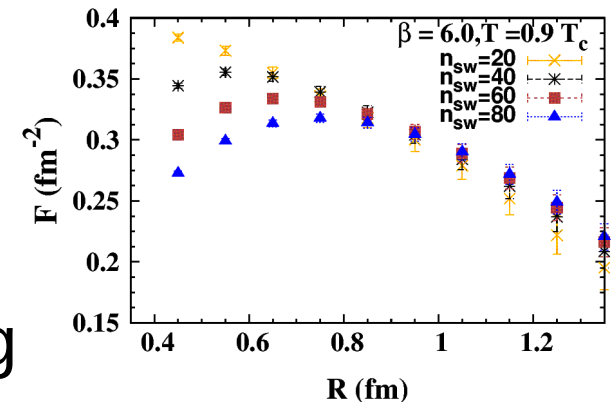
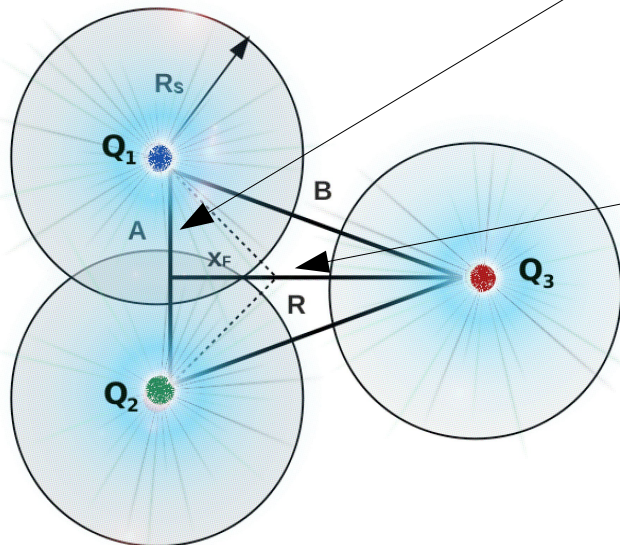
Smearing Radius

$A=0.6$ fm

To ensure minimal effect of 4 -D smearing on the 3Q potential the smearing Sphere around each quark should be Non-overlapping.

$A=0.8$ fm

$A=1.0$ fm



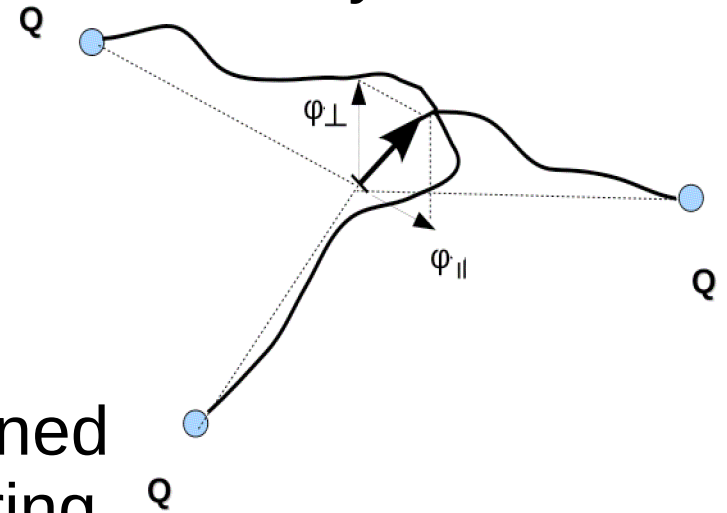
Baryonic String Model

In the Y-baryonic string model, the elementary constituents of hadronic matter (quarks) are confined together due to formation of very thin flux tubes.

The quarks are connected by three strings that meet at a junction, the *Y-string configuration* is expected to be the dominant configuration in the IR region of the baryon.

The classical configuration is the one that minimizes the area of the string world sheets.

The position of the junction is determined by the requirement of minimal total string length.



Baryonic string models

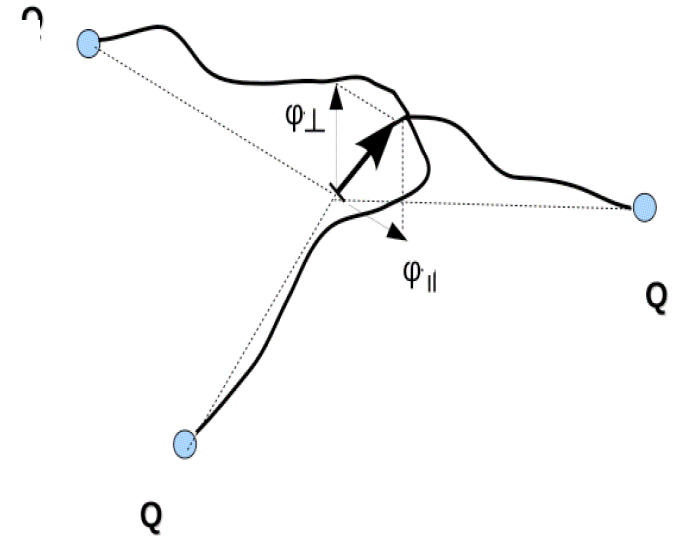
The first test of the baryonic string model predictions with LGT at zero temperature (3 Potts model) for three quark potential has been reported by DeForcrand and Jahn. (verification of Luscher Like term) **Ph. De Forcrand and O. Jahn, N phys A 755(2005)**

Pfufner, Bali, and Panero **PhysRevD.79.025022** extended the calculations of the above model to the thickness of the fluctuating baryonic junction

They have shown a logarithmic growth of the junction width.

$$\langle \varphi_{\perp}^2 \rangle = \frac{2}{L_T} \sum_{w>0} \frac{1}{m w^2 + \sigma w \sum_i \coth(w L_i)}$$

with $w = 2\pi n/L_T$.



Expanding the NG action around the equilibrium configuration yields

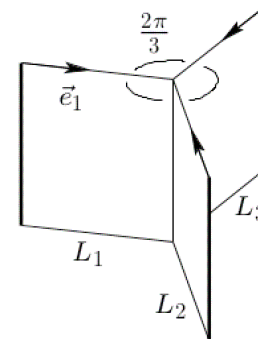
$$S = S_{\parallel} + \frac{\sigma}{2} \sum_{a,i} \int_{\Gamma_a} d^2\zeta \frac{\partial \xi_a}{\partial \zeta_i} \cdot \frac{\partial \xi_a}{\partial \zeta_i} + m \left(T + \frac{1}{2} \int_0^T dt |\dot{\varphi}|^2 \right), \quad (1)$$

where again ζ_1, ζ_2 are world sheet parameters and

$$S_{\parallel} = \sigma \sum_a \left(L_a T + \int dt \mathbf{e}_a \cdot \varphi(t) \right) = \sigma L_Y T. \quad (2)$$

$L_Y = \sum_a L_a$ above denotes the total string length.
 $\sum_a \mathbf{e}_a = 0$.) In the $T \rightarrow \infty$ limit

Classical ground state: minimal area \Rightarrow "Y configuration"



junction at Steiner point:

$$\sigma \sum_{\alpha=1}^3 \vec{e}_{\alpha} = 0$$

$$\Rightarrow \angle(\vec{e}_{\alpha}, \vec{e}_{\beta}) = \frac{2\pi}{3}.$$

⏪ ⏩ ⏴ ⏵ ⏶ ⏷ ⏸ ⏹ ⏺ ⏻ ⏼ ⏽ ⏾ ⏿ ⏿ \rightsquigarrow "Y law": $V_{\text{cl}} = \sigma_{\text{meson}} \underbrace{(L_1 + L_2 + L_3)}_{L_Y}$

We are interested in the expectation value

$$\langle \varphi^2 \rangle = \langle \varphi^{\perp 2} \rangle + \langle \varphi^{\parallel 2} \rangle = \frac{I_{\perp}}{I_1} + \frac{I_{\parallel}}{I_2}, \quad (1)$$

where

$$I_{\perp} = \int D\varphi^{\perp} \varphi^{\perp 2} \exp \left\{ -\frac{1}{2} \sum_w \left[mw^2 + \sigma w \sum_a \coth(wL_a) \right] \times |\varphi_w^{\perp}|^2 \right\}, \quad (2)$$

$$I_{\parallel} = \int D\varphi^{\parallel} \varphi^{\parallel 2} \exp \left\{ \sum_w \left[-\frac{1}{2} \left(mw^2 + \sigma w \sum_a \coth(wL_a) \right) \times |\varphi_w^{\parallel}|^2 + |\varphi_{w,x}^{\parallel}|^2 A_x + |\varphi_{w,y}^{\parallel}|^2 A_y + |\varphi_{w,y}^{\parallel}|^2 A_y + 2 \left(\text{Re}(\varphi_{w,x}^{\parallel}) \text{Re}(\varphi_{w,y}^{\parallel}) + \text{Im}(\varphi_{w,x}^{\parallel}) \text{Im}(\varphi_{w,y}^{\parallel}) \right) A_{\text{Re}} \right] \right\}. \quad (3)$$

The Conformal mapping

Jahn and De Forcrand calculated the baryonic potential, by evaluating the determinant of the Laplacian based on conformally mapping generalized domains of the blade (corresponding to each string) to rectangles.

O Jahn and Ph. Deforcrand, hep-lat/0209062, Ph. De Forcrand and O. Jahn, N phys A 755(2005)

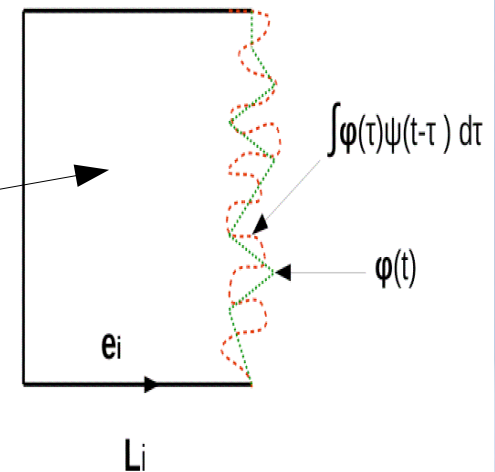
This is done after regularization, by Conformally mapping a rectangle to fluctuating blade.

$$f_{\alpha}(z) = z + \frac{1}{\sqrt{T}} \sum_{\omega=0} \frac{e_{\alpha} \cdot \varphi_{\omega}}{\sinh(\omega L_{\alpha})} e^{\omega z}$$



The general domains Γ_a describing the world sheet of each blade can now be described with the aid of the convoluting scalar function ψ such that the conformal mapping to a rectangle is

$$f_i(z) = z + \frac{1}{\sqrt{L_T}} \sum_{\omega=0} e_{k \cdot \varphi_\omega} \frac{\psi(\omega, L_i)}{\sinh(\omega L_i)} e^{\omega z}. \quad (1)$$



The integration over Fourier modes of the fluctuating junction ϕ can be performed in a similar way as detailed in Ref. [?].

The mean-square width of the perpendicular fluctuation of the junction acquires a simple modification after solving for the position of the junction $\xi_{min,i}$ for each blade with the convoluted position

$$\xi_{min,i} = \frac{1}{\sqrt{L_T}} \sum_w \varphi_{w,\perp i} \psi(w, L_i) \frac{\sinh(ws)}{\sinh(wL_i)} e^{iwt}. \quad (2)$$

Junction Fluctuations at finite temperature

Smoothing scalar can be found from the mesonic limit.

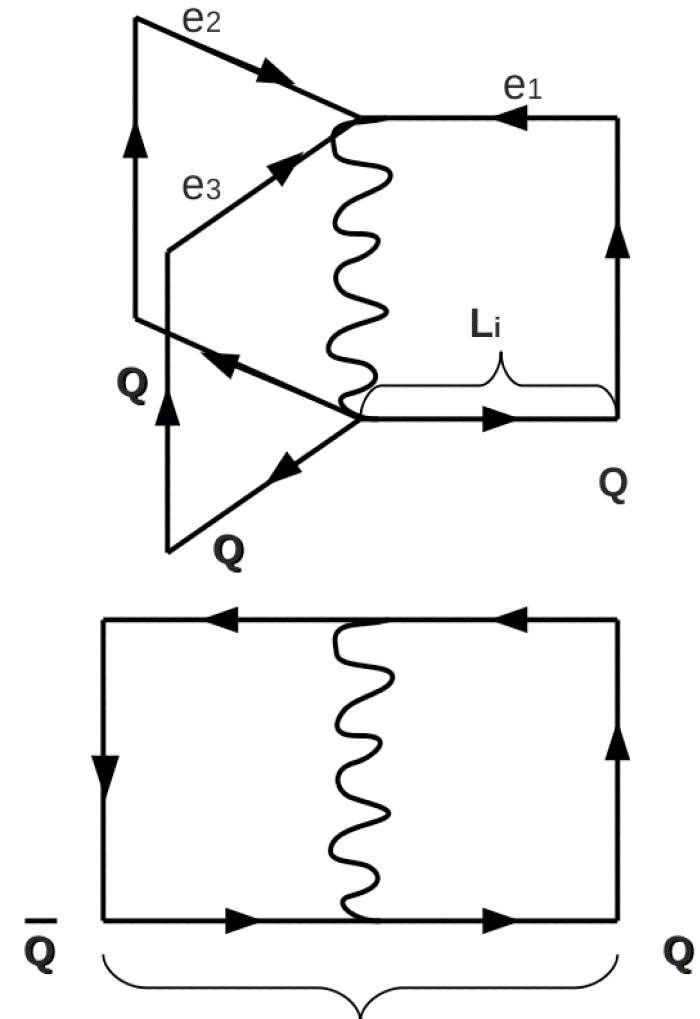
$$h(t) = \int_{-\infty}^{\infty} \phi(\tau) \psi(t - \tau) d\tau$$

The action is given by,

$$S = S_{||} + \frac{\sigma}{2} \sum_{a,i} \int_{\Gamma_a} d^2\zeta \frac{\partial \eta_a}{\zeta_i} \cdot \frac{\partial \eta_a}{\partial \zeta_i} +$$

$$m(T + \frac{1}{2} \int_0^T dt \int_0^{\infty} |\dot{h}(t)|^2),$$

$$w^2(\xi_1, \tau) = \frac{1}{2\pi\sigma} \log\left(\frac{R}{R_0}\right) + \frac{1}{2\pi\sigma} \log\left| \frac{\theta_2(\pi \xi_1/R; \tau)}{\theta_1'(0; \tau)} \right|$$



Width of the junction_

Following the same procedure as PhysRevD.79.025022 for the calculation of the thickness of the junction, this results in a simple modification for the perpendicular fluctuations to (Pfufer, Bali, and Panero)

$$\langle \varphi_{\perp}^2 \rangle = \frac{2}{L_T} \sum_{w>0} \frac{1}{mw^2 + \sigma w \sum_i \coth(wL_i) \psi(w, L_i)}. \quad (1)$$

The form of this convoluting scalar can be derived from the mesonic limit.

$$\psi(w, L_i) = \frac{-kw}{2\sigma \coth(wL_i)} - \frac{(wL_T - \pi)}{2wL_T \coth(wL_i)} \left(\frac{2L_i \chi(\tau_i) + 1}{2L_i \chi(\tau_i) - 1} \right)^{wL_T/\pi - 1} \quad (2)$$

$$\text{with } \chi(\tau) = \frac{\theta_2(0; \tau)}{\theta_1'(0; \tau)}.$$

As indicated above, the parameter m shifts the mean-square width of the fluctuations by a constant. The parameter m can be chosen such that R_0 cancels out from both sides.

(b) In-plane after orthogonalization and including thermal corrections would read:

$$\langle \varphi_{x,\parallel}^2 \rangle = \frac{2}{L_T} \sum_{w>0} \frac{1}{A_{x,w} + A_{y,w} - (A_{xy,w}^2 + (A_{x,w} - A_{y,w})^2)^{1/2}},$$

$$\langle \varphi_{y,\parallel}^2 \rangle = \frac{2}{L_T} \sum_{w>0} \frac{1}{A_{x,w} + A_{y,w} + (A_{xy,w}^2 + (A_{x,w} - A_{y,w})^2)^{1/2}}.$$

Where A_x , A_y and A_{xy} are defined as

$$A_x = \left(mw^2 + \sigma w \sum_i \coth(wL_i) \psi(w, L_i) + \frac{\sigma}{2} w + \frac{(D-2)w^3}{24\pi} \right) \left[\sum_a e_{a,x}^2 \coth(wL_a) \right],$$

$$A_y = \left(mw^2 + \sigma w \sum_i \coth(wL_i) \psi(w, L_i) + \frac{\sigma}{2} w + \frac{(D-2)w^3}{24\pi} \right) \left[\sum_a e_{a,y}^2 \coth(wL_a) \right],$$

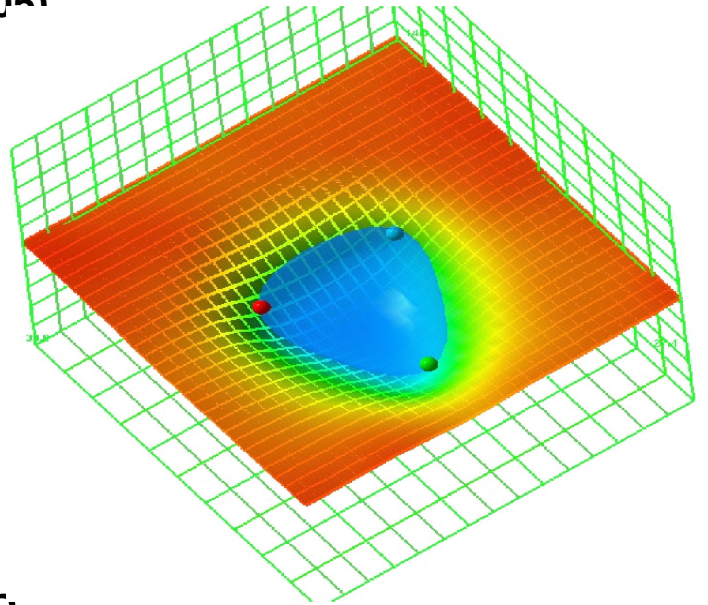
$$A_{xy} = \left(\frac{\sigma}{2} w + \frac{(D-2)w^3}{24\pi} \right) \left[\sum_a e_{a,x} e_{a,y} \coth(wL_a) \right].$$

Lattice Results

Lattice QCD findings regarding the 3-quark potential are settled about a confining potential that admits two possible models depending on the inter-quark separation distances:

3Q Potential

The so-called Delta parametrization for small quark separation distances of $R < 0.7$ fm and the Y-ansatz for $0.7 < R$ fm. Ph. De Forcrand and O. Jahn, N phys A 755(2005)

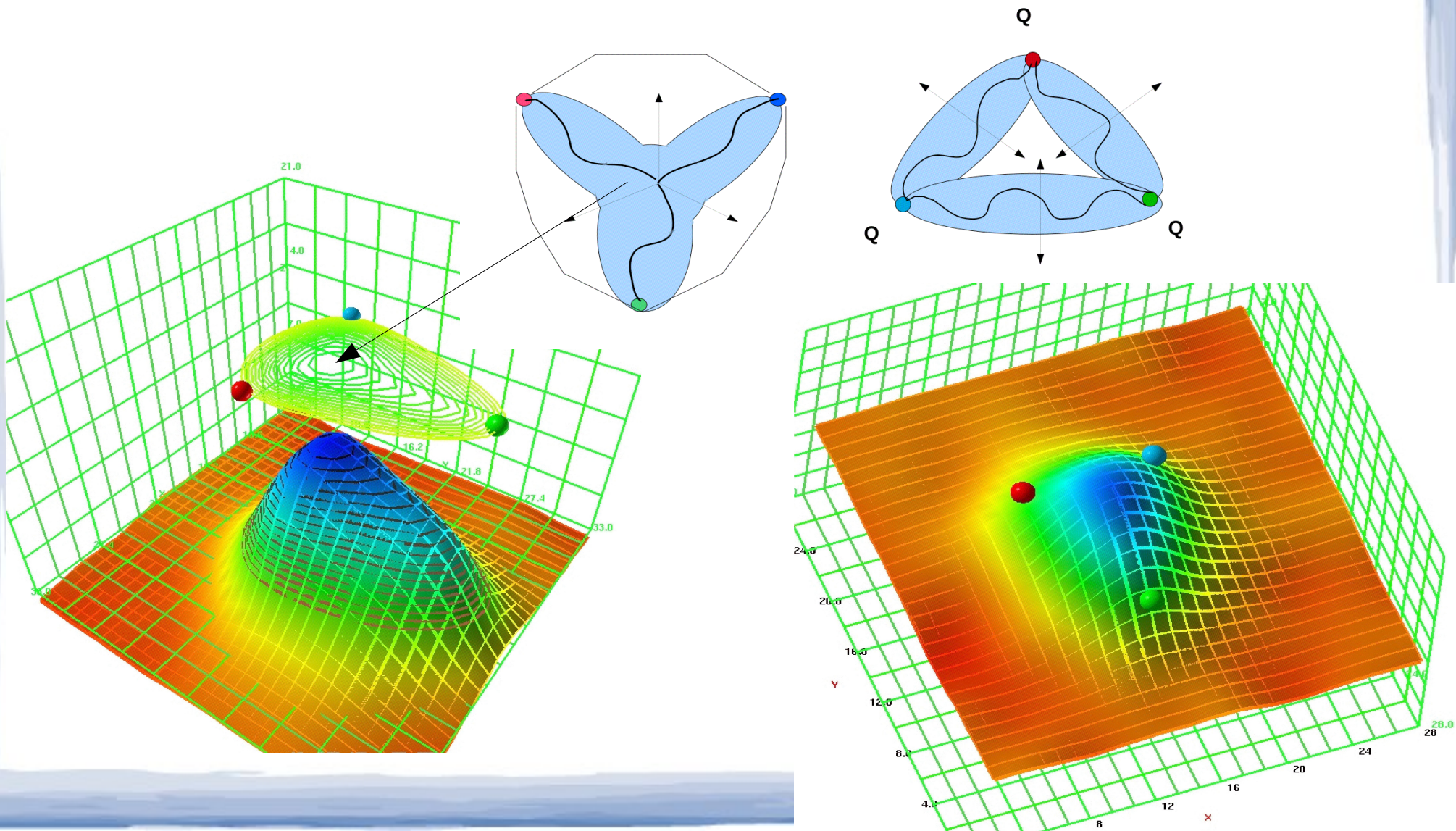


Gluonic distribution

The revealed flux distributions displays an action-density profile consistent with a filled Delta shape iso-surface. (even at large distances) up to $R = 1.3$ fm.

Y-String signatures: a) filled Delta-shaped

The action density does not look like a flux tube that form around the perimeter of the triangle. The distribution maximum is inside the triangle.

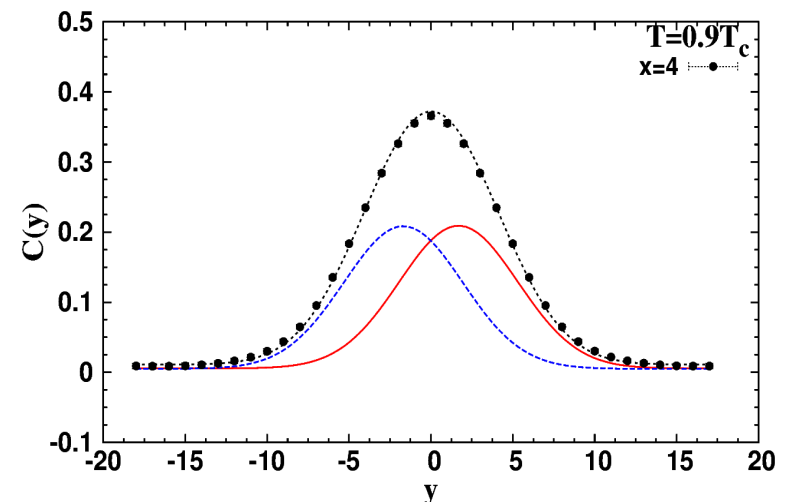


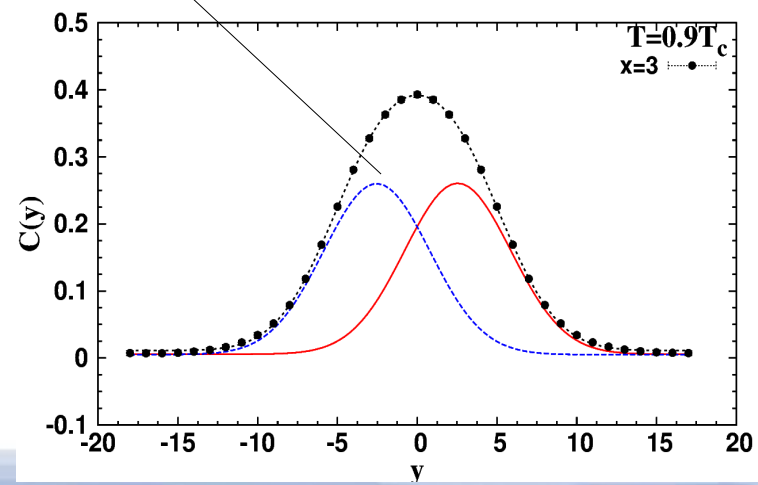
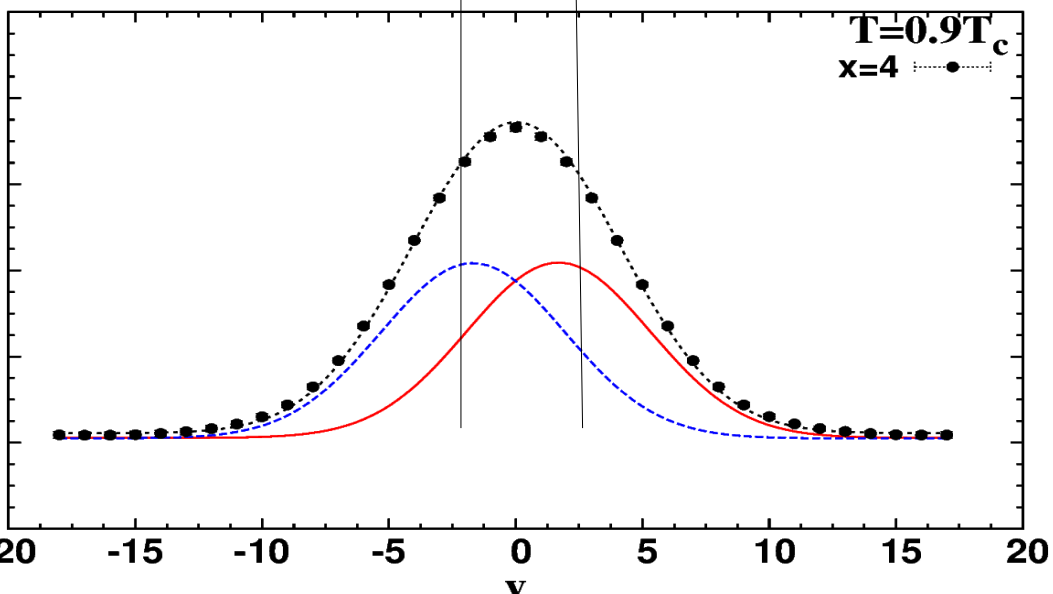
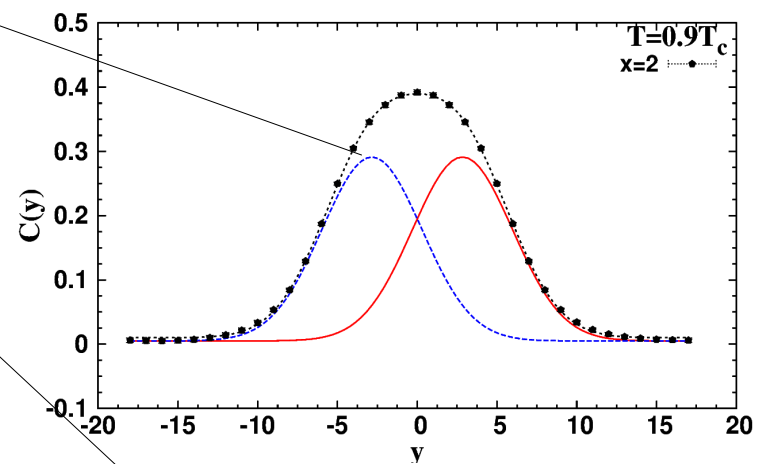
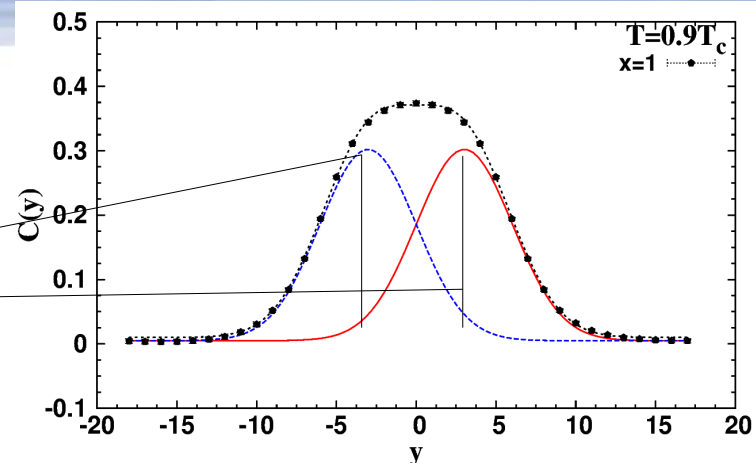
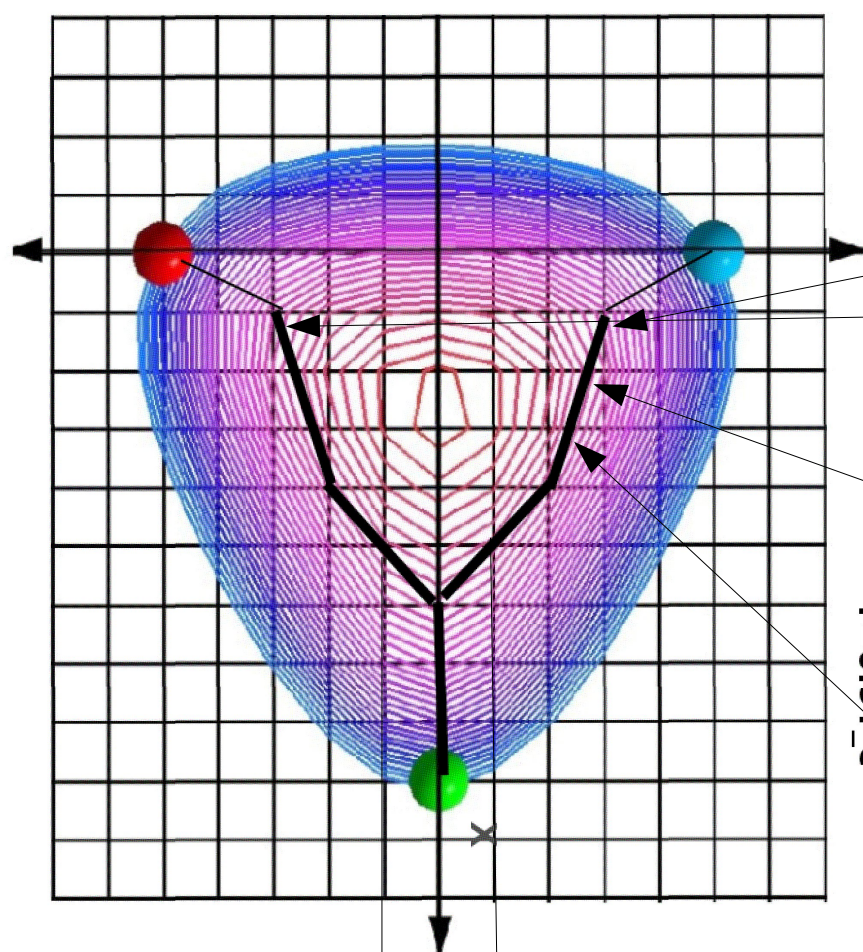
Y-String signatures: b) Two-Gaussian Distribution

In the meson a single Gaussian corresponds to the profile of one single string.

In the Baryon, our results show that the action density profile well fits to a two Gaussian form.

$$G(y; a, w) = A \exp(-(y-u)^2/W^2) + A \exp(-(y+u)^2/W^2)$$

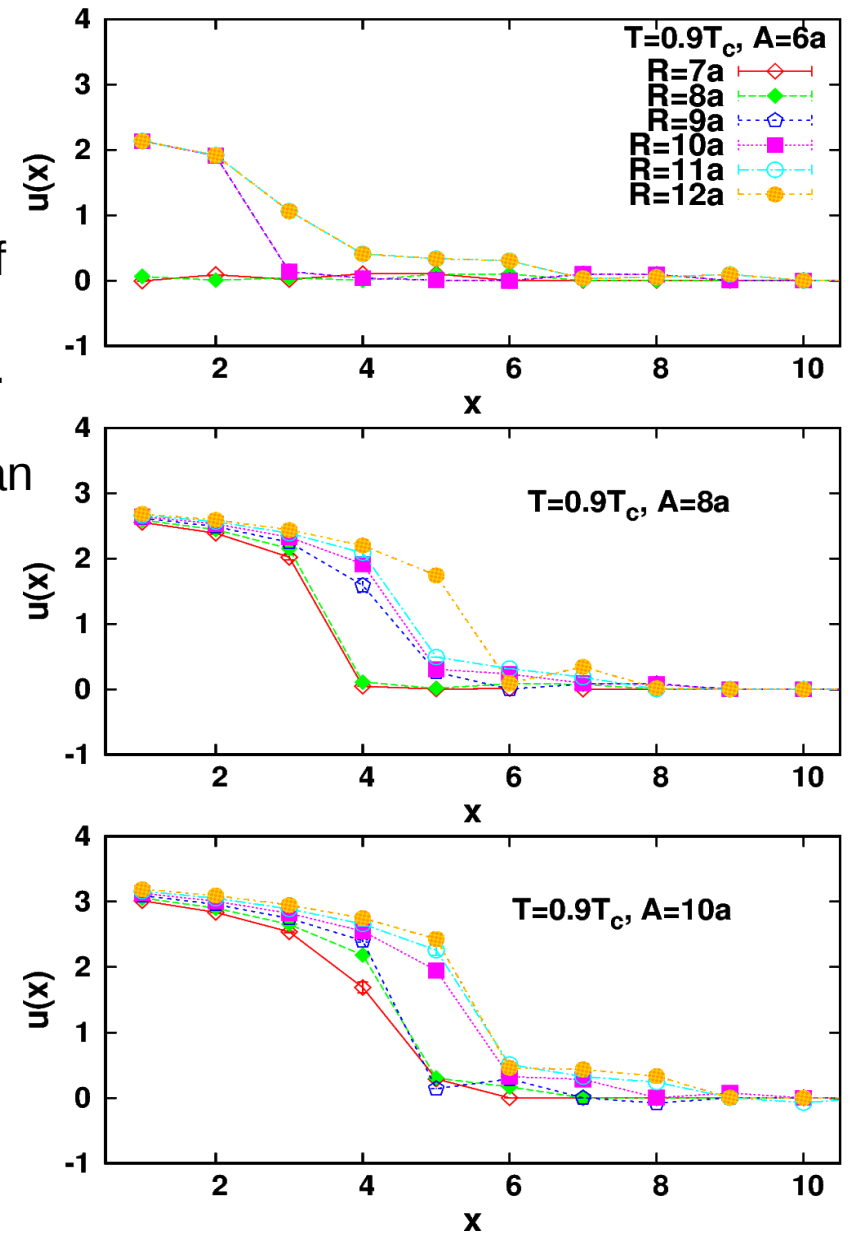
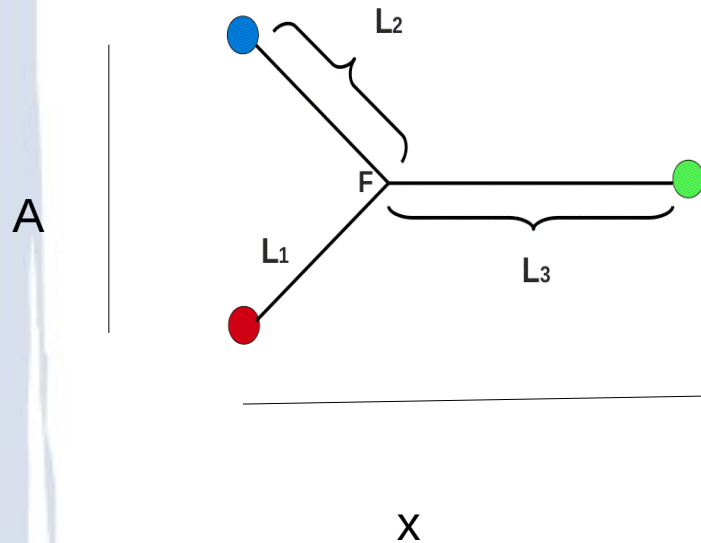


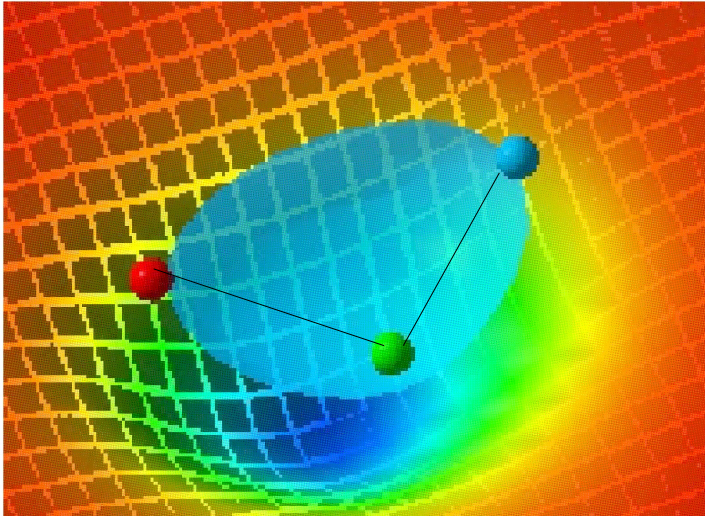


The two Gaussian Profile

The plots shows how the separation between the two Gaussians varies with the movement of third quark at the top of the triangle and with the change of the length of the triangle base A.

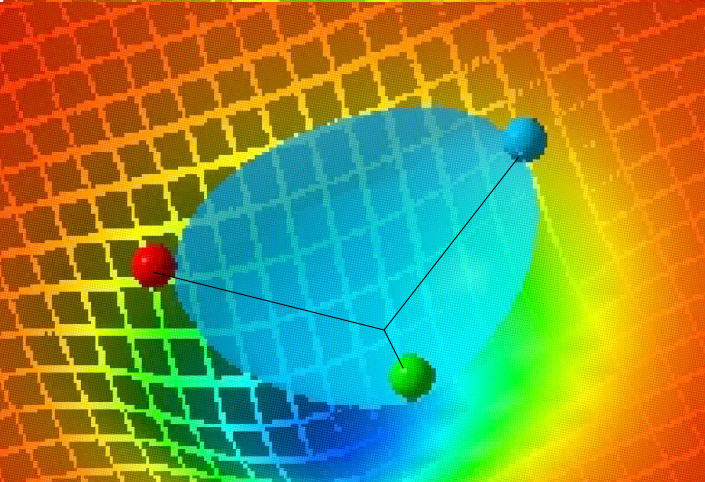
We call the position x , at which $u(x)=0$, the mean Position of the junction.



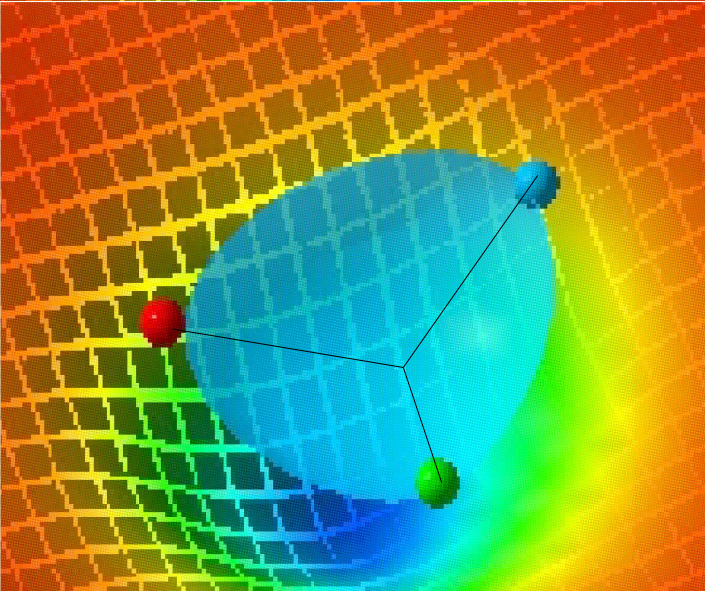


This a schematic plot of the profile of the two Gaussians Superimposed over the rendered action density.

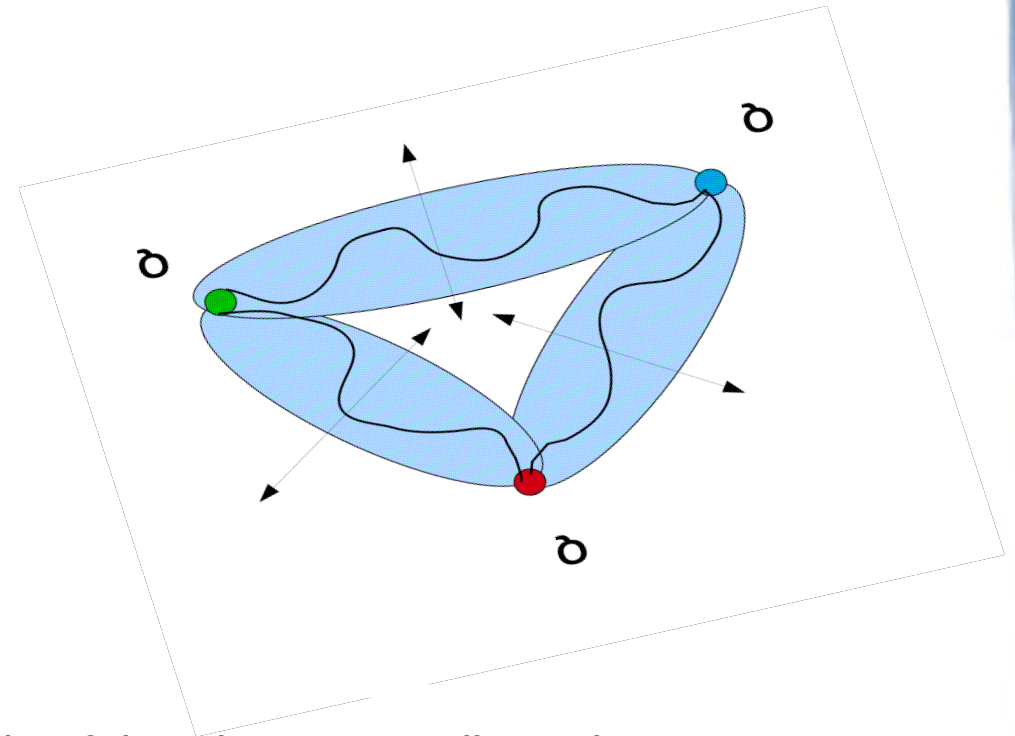
$R= 0.3 \text{ fm}$



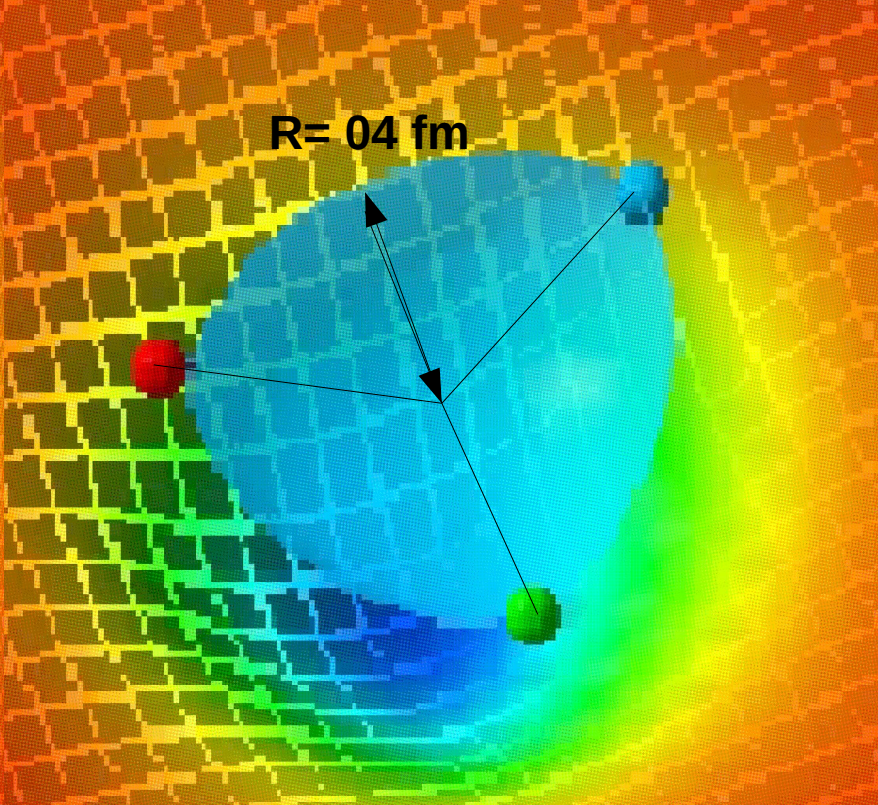
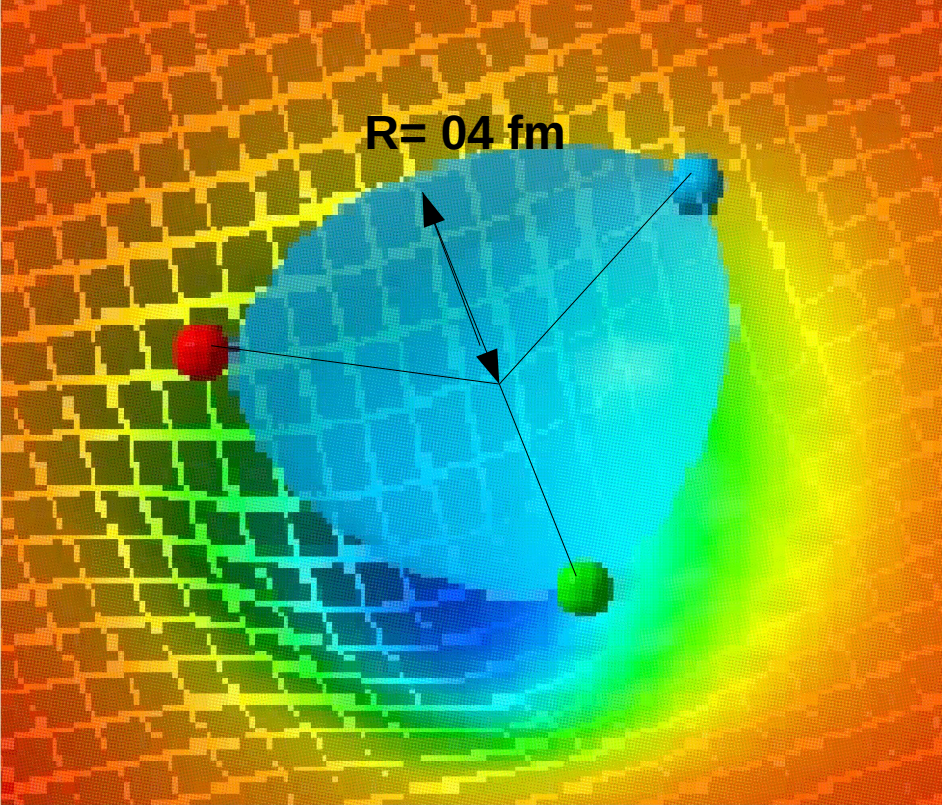
$R= 0.4 \text{ fm}$



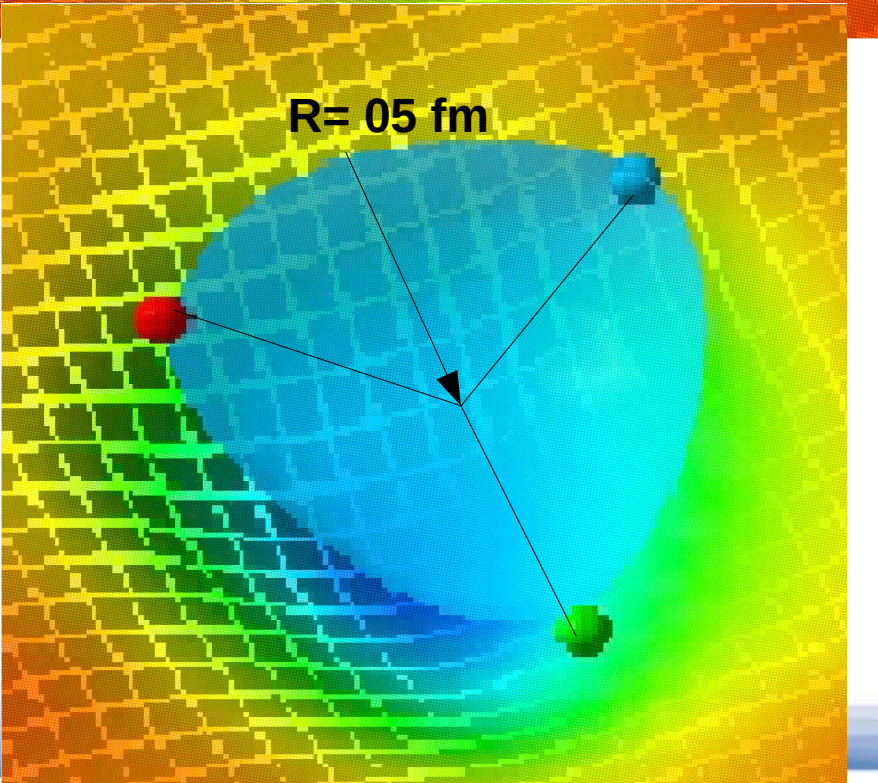
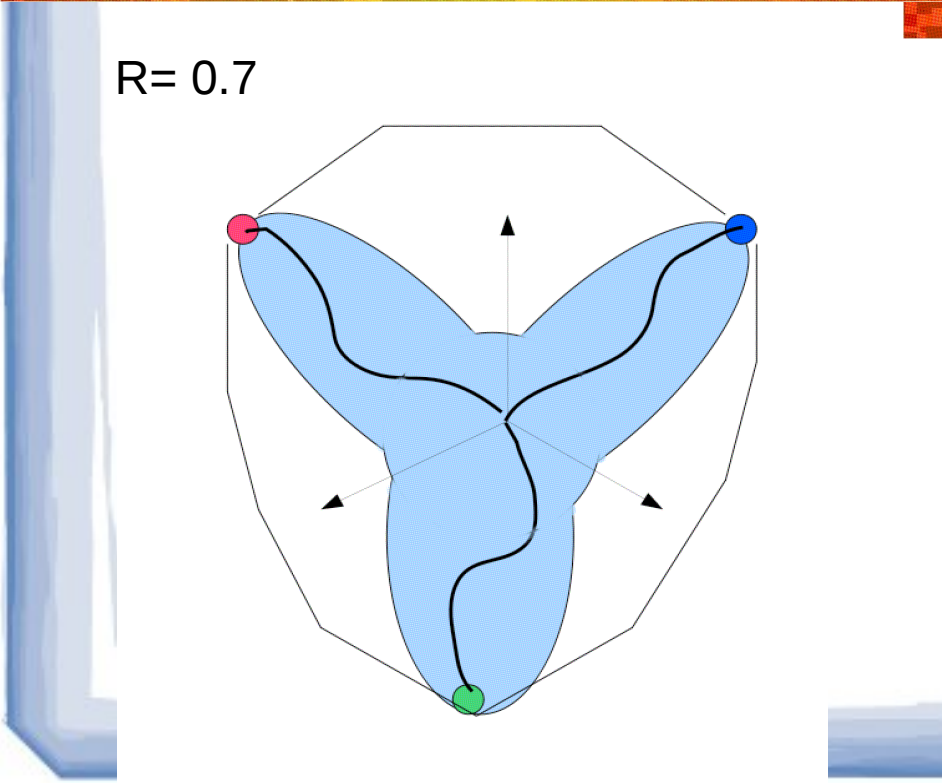
$R=0.5 \text{ fm}$



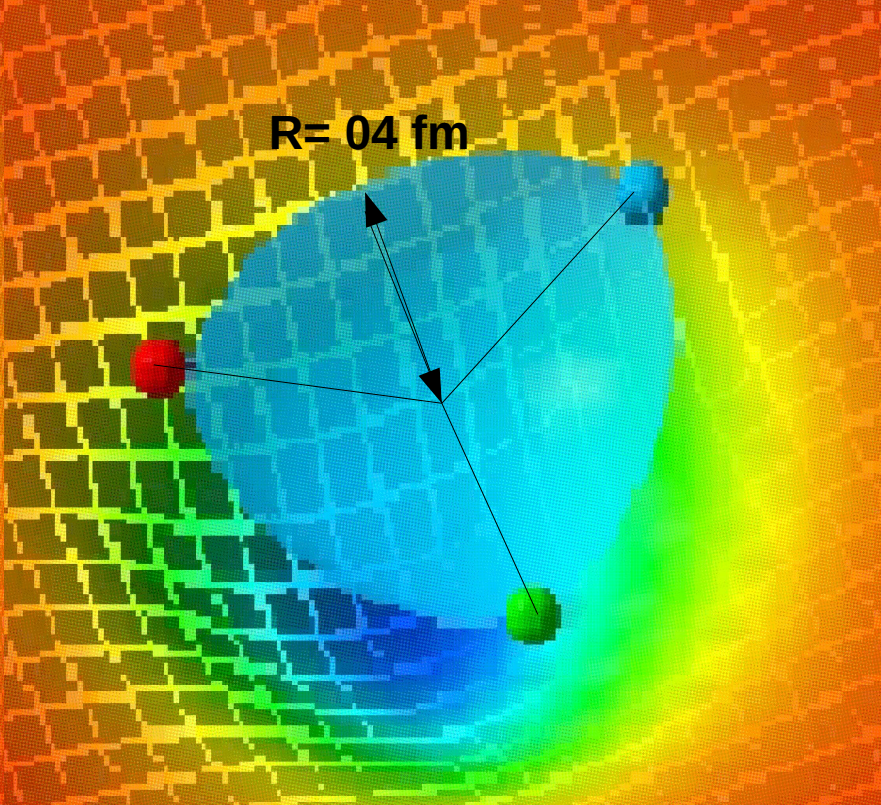
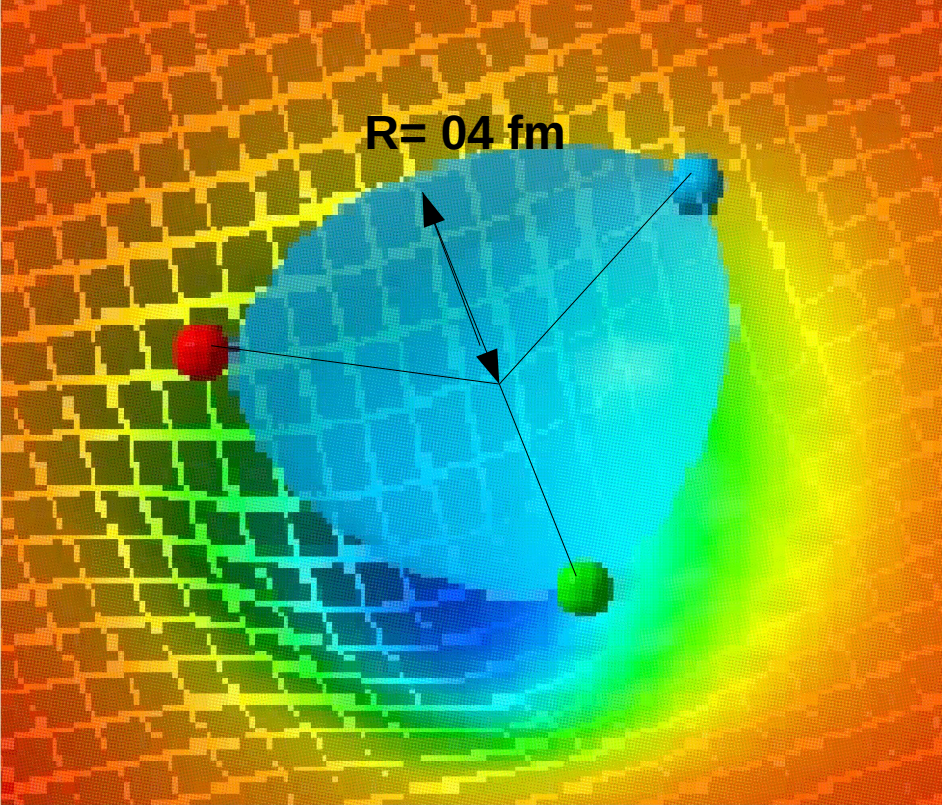
The profile of the trings at small quark separation looks like a Delta shape.



$R = 0.8 \text{ fm}$

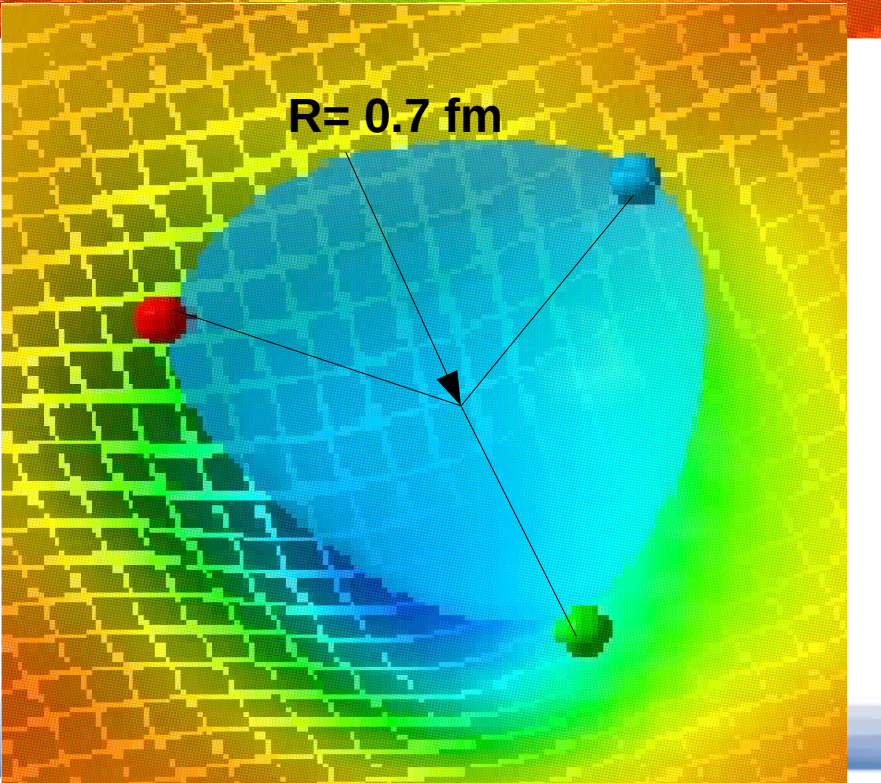
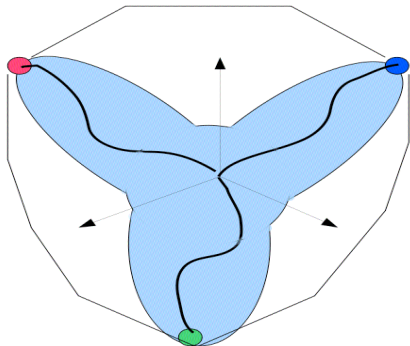


$R = 1.0 \text{ fm}$



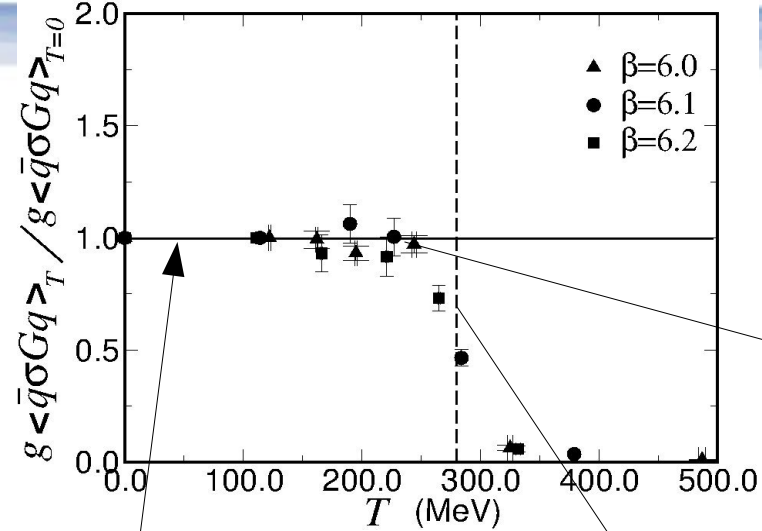
R=0.8 fm

The profile at larger quark separation is Y-shaped.



R=1.0 fm

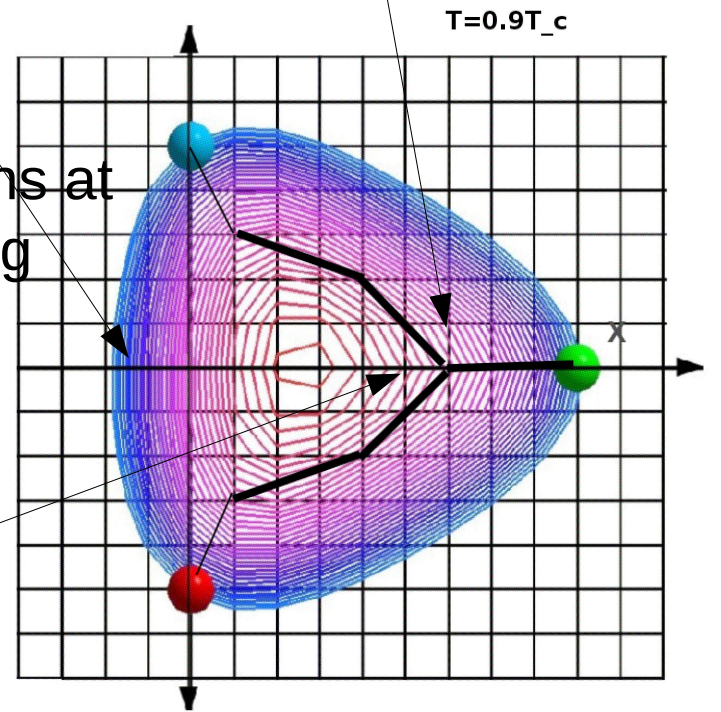
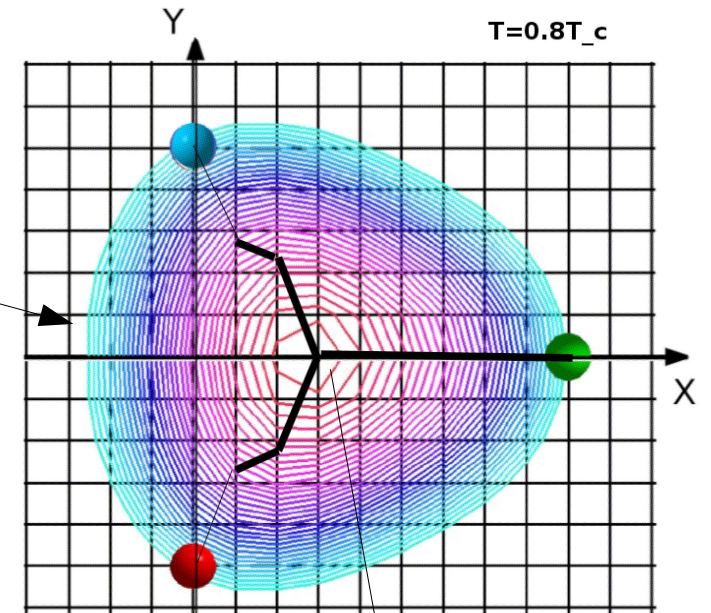
R= 0.7 fm



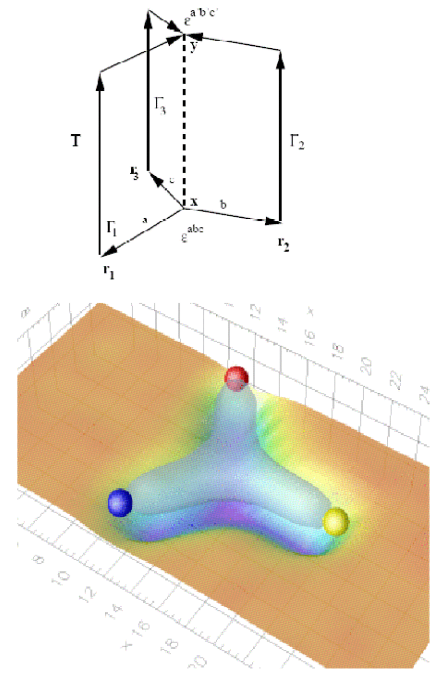
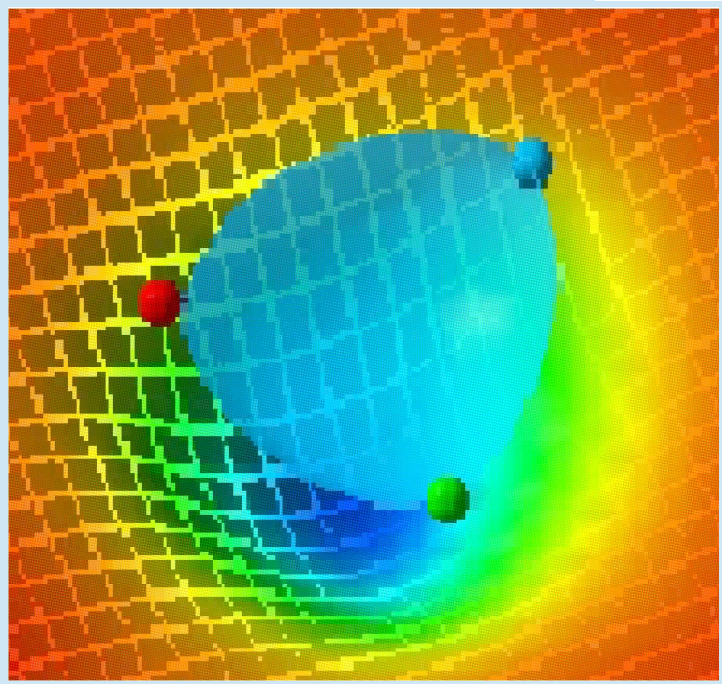
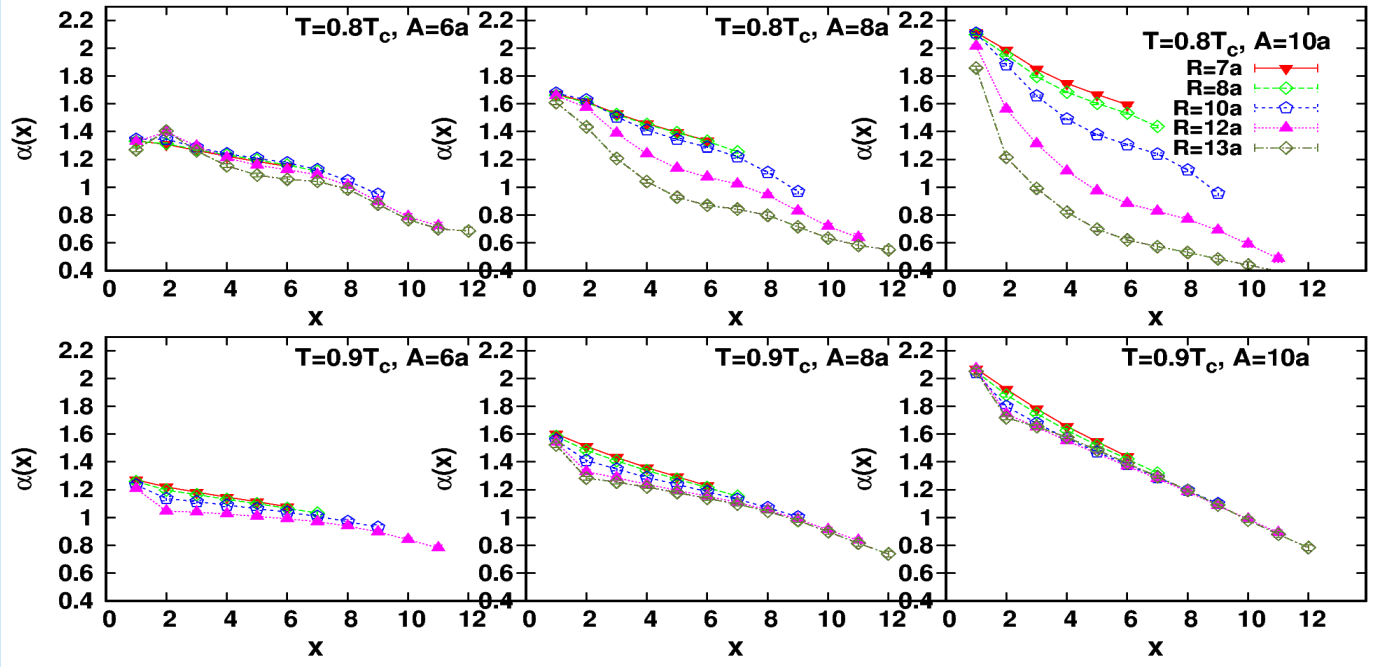
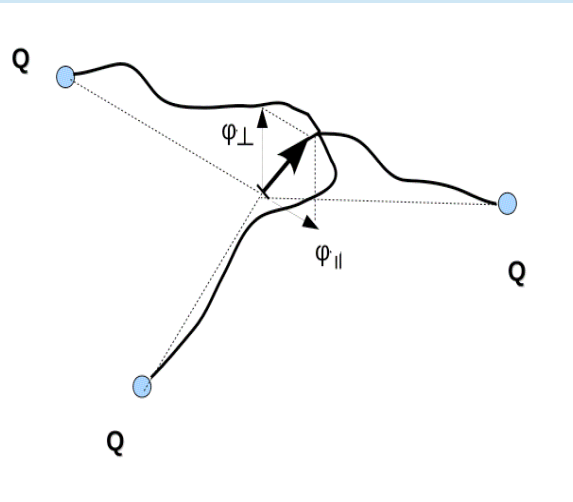
The change in string tension with temperature near the end of QCD plateau is roughly 10%.

The revealed color map in mesons and baryons at this temperature can be speculated as exhibiting similar behaviour to that at zero temperatures.

The movement of the junction with the increase of the temperature.



Aspect ratio Wz/Wx



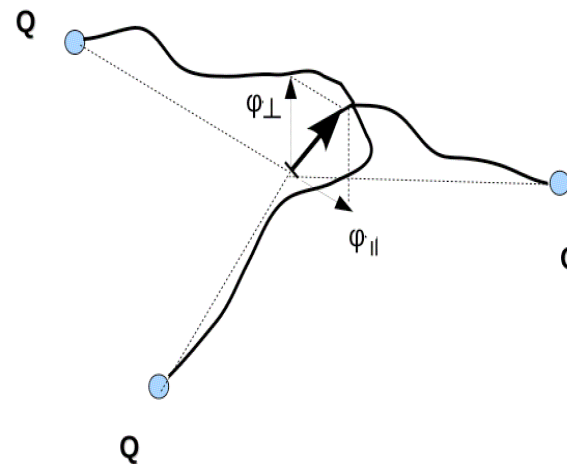
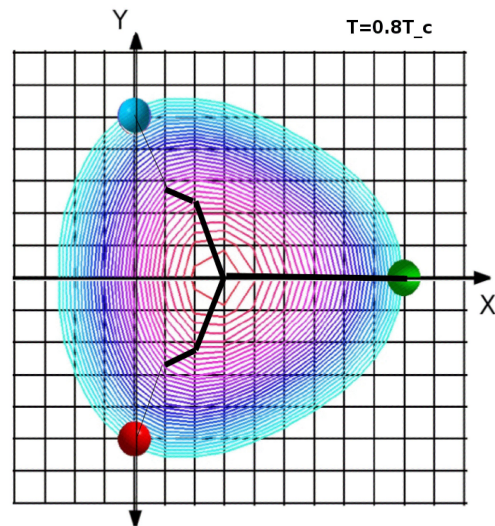
Qualitative properties

- Filled Delta Shape Flux profile.
- Underlying structure of Y-shaped Gaussian string profile.
- Minimal length for the Y-Profile at the end of QCD plateau, Maximum near deconfinement point.
- Aspect ratio greater than 1, indicating a larger restoring force in the quark plane.

Lattice data versus String Model

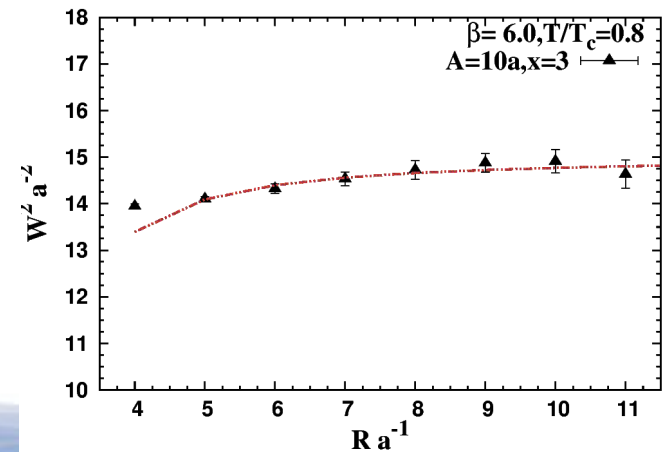
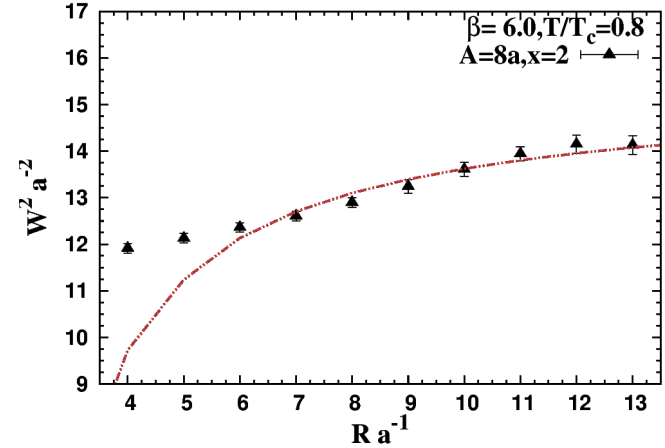
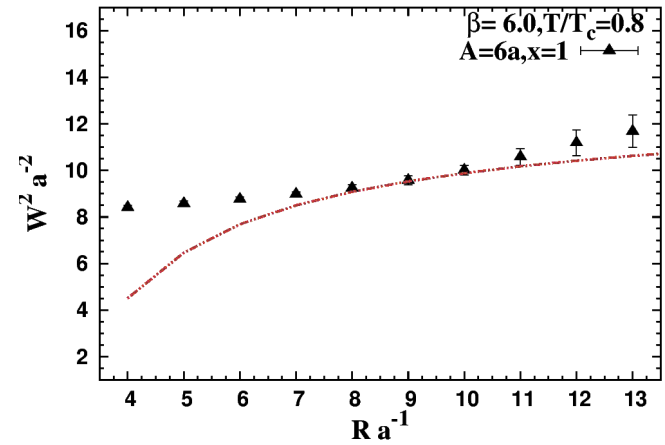
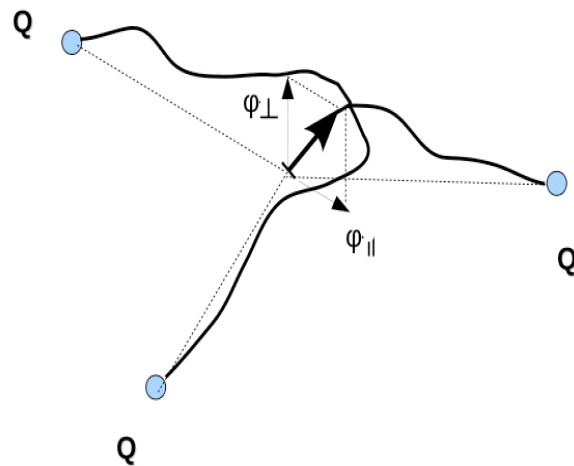
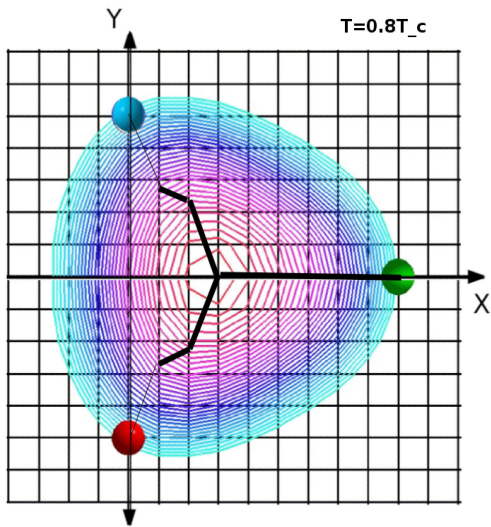
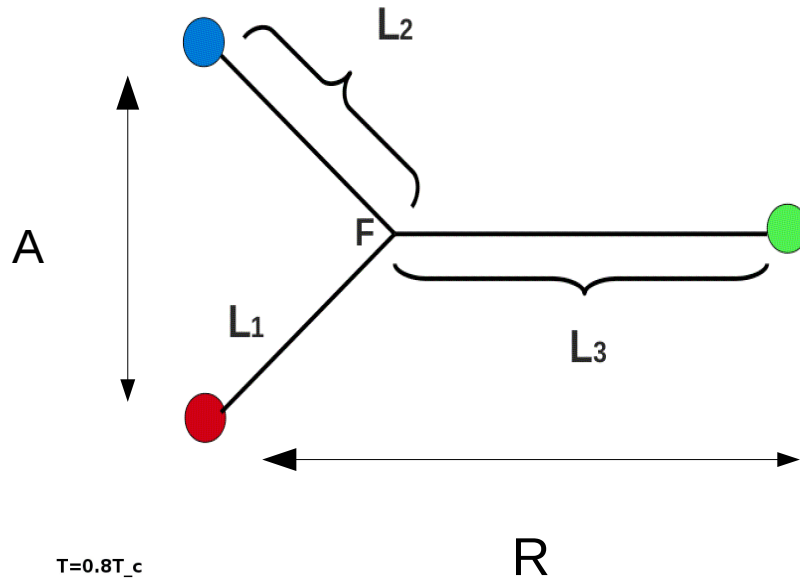
The broadening of the flux tube with the increase of the source separation is compared to the corresponding string model predictions.

This can provide a first indication of the compatibility of the baryonic string model with the measured LGT junction profile, the position of the junction and its proposed insight.



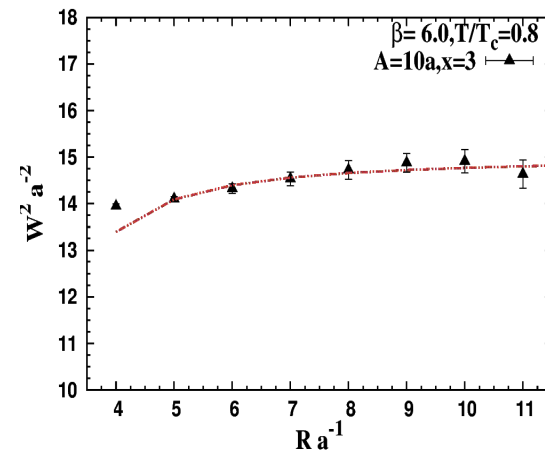
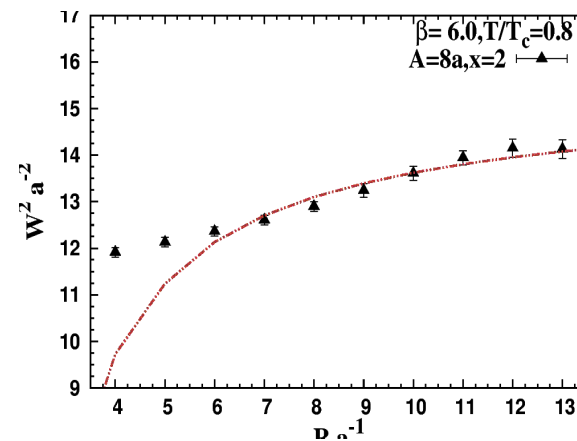
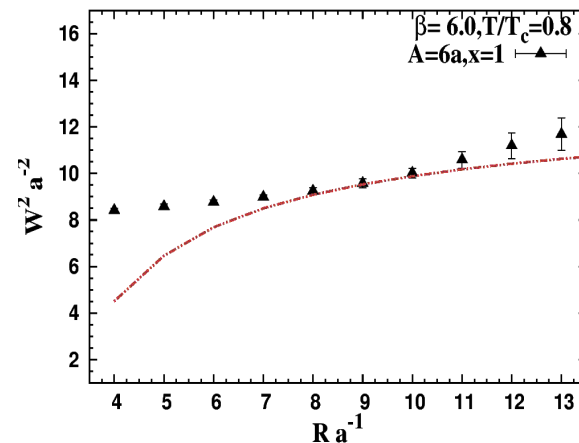
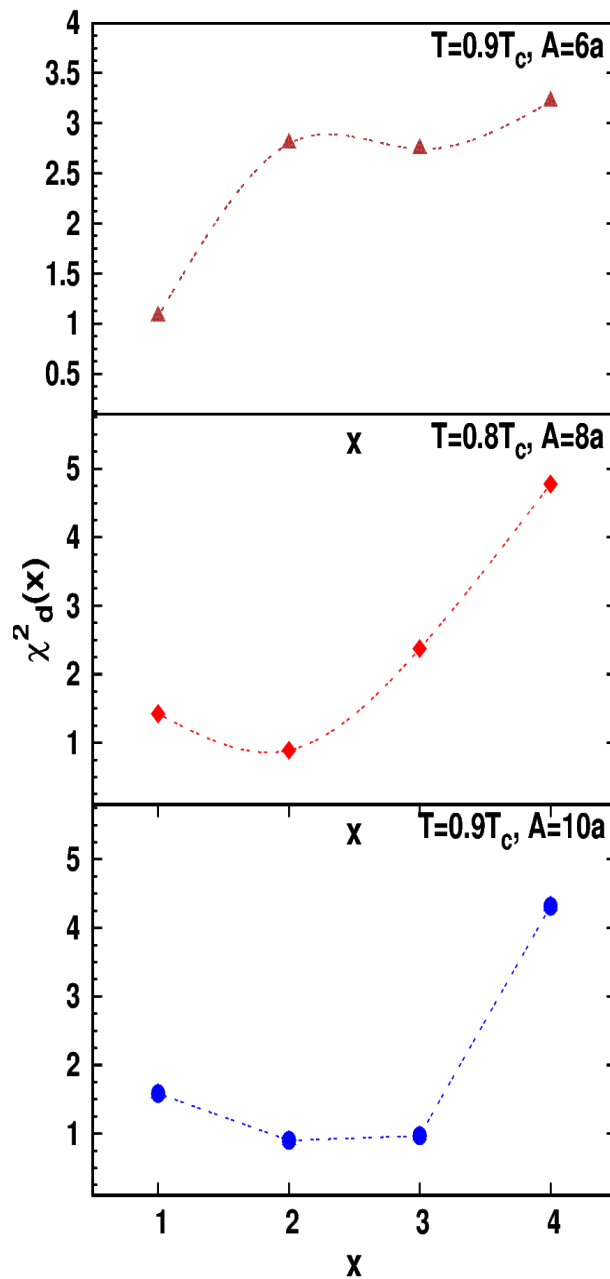
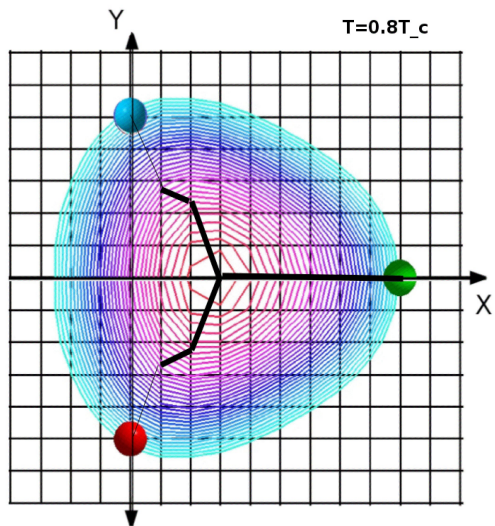
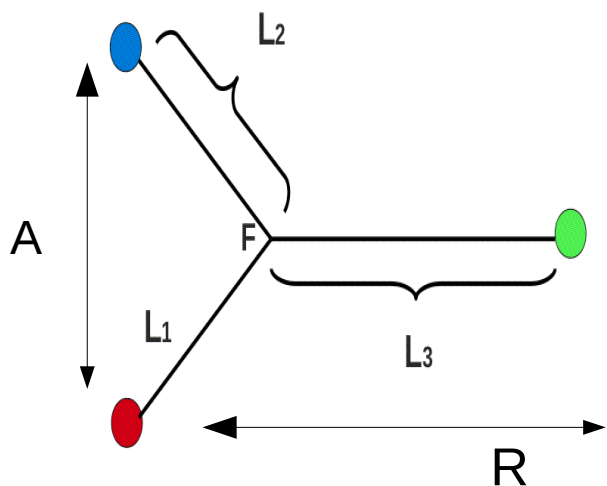
Returned fits of the gluon flux to stringa width profile

a) In-plane Fluctuations



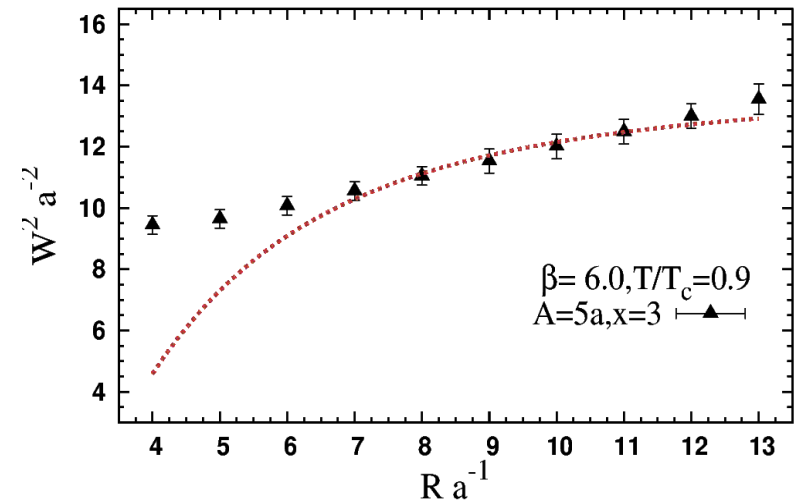
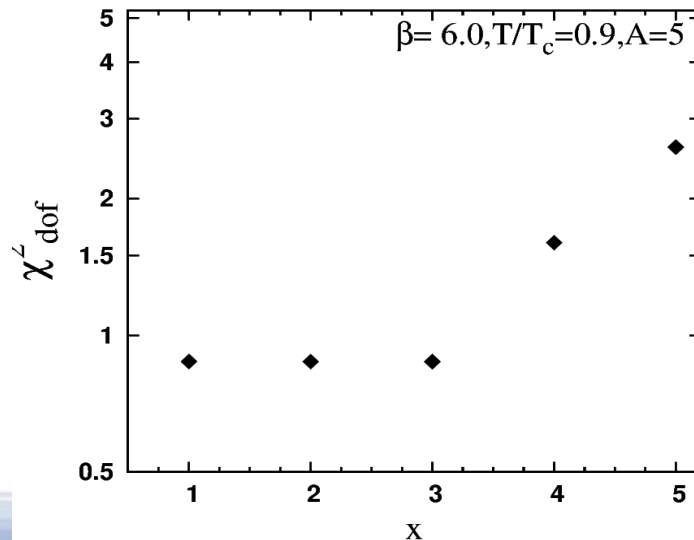
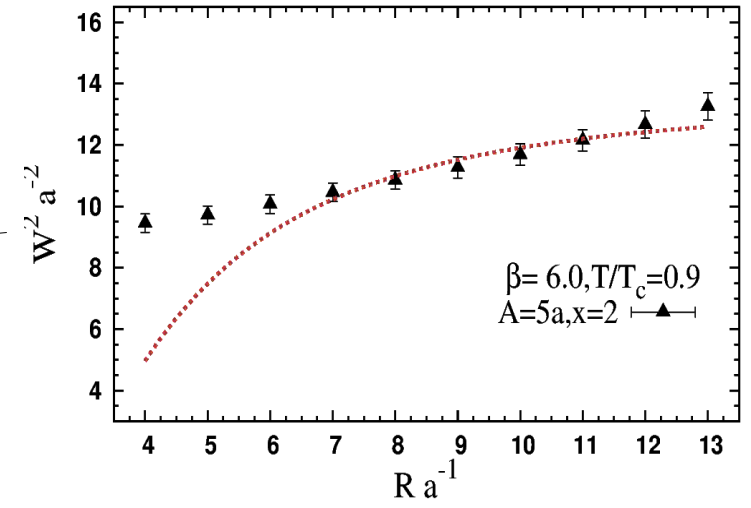
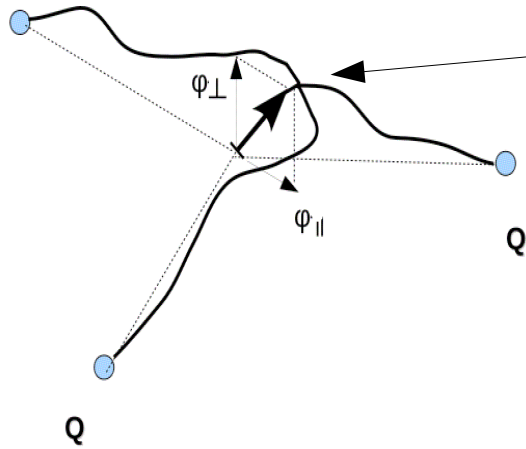
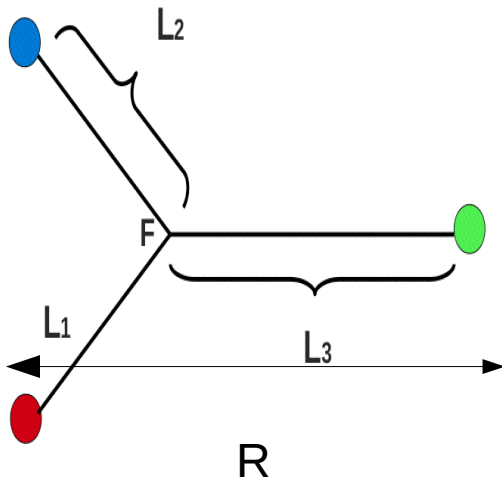
Returned fits of the gluon flux to string width profile

a) In-plane Fluctuations



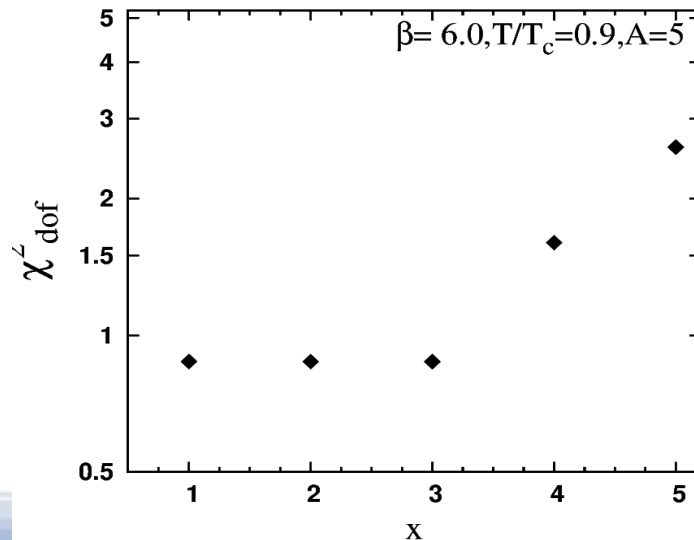
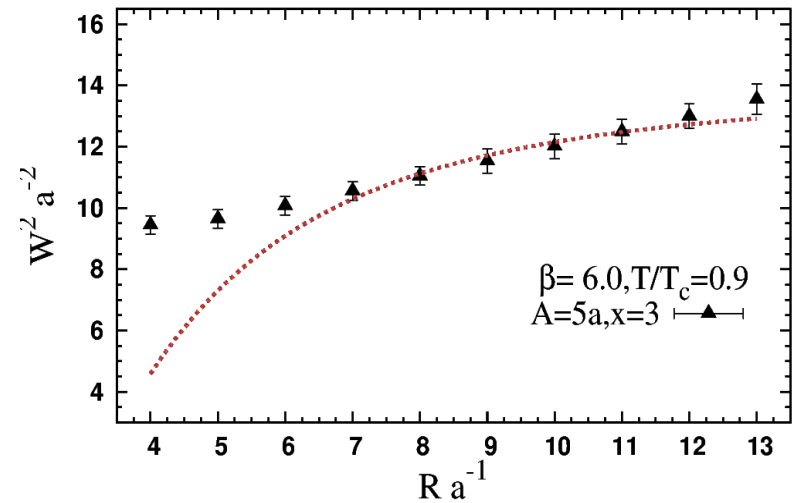
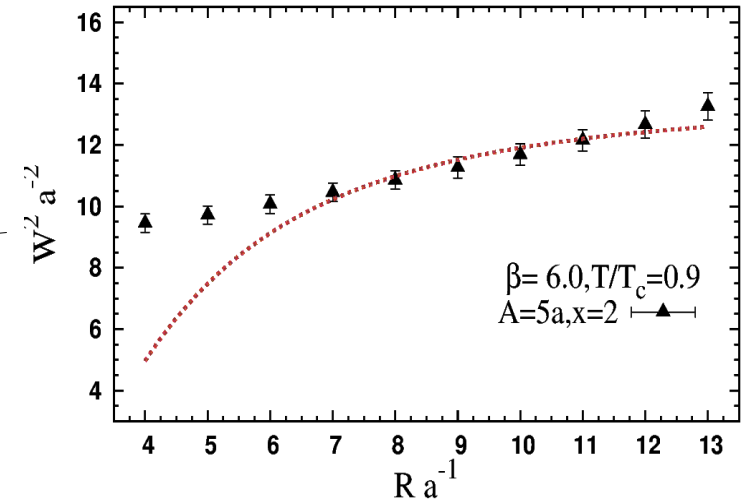
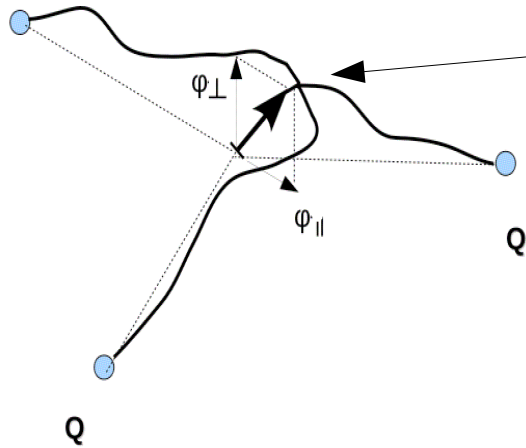
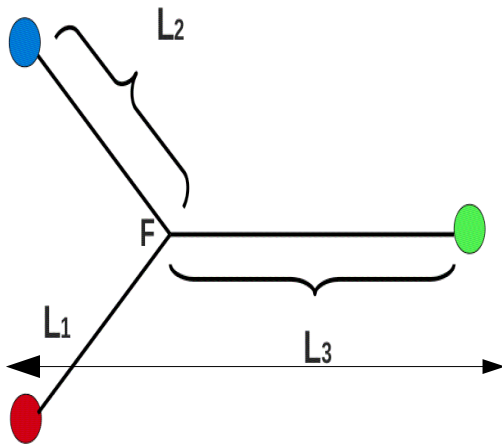
Returned fits of the gluon flux to Y-string width profile

b) Perpendicular Fluctuation



Returned fits of the gluon flux to Y-string width profile

b) Perpendicular Fluctuation



Conclusion

- The signatures of the baryonic string has been identified in the qualitative properties of the energy profile and directly via fit behaviour of a form consisting of a sum of two-Gaussian.
- The Y-baryonic string model has been discussed at high temperature for the Width profile of the junction.
- The lattice data for the mean-square width of the gluonic action density has been compared to the corresponding width calculated based on string model at finite temperature.
- The best fits for the string model are returned for large quark source separation $R > 0.8$ fm. Only assuming the classical position of the strings at the Fermat point of the configuration (point that minimizes the length of Y-strings).
- In this analysis, it is the first time we can directly look and identify a clear formation of Y-shaped confining strings in the baryonic filled Δ -shaped action.
- The revealed form of the flux in the baryon presents a potential candidate for the exact geometry of the flux-tubes at zero temperature.

Prospective:-

Extending the calculations to zero temperature

- Noise reduction: Noise reduction by combining smearing with multi-level integration methods. Ahmed S. Bakry, Xurong Chen, Pengming Zhang. International Journal of Modern Physics E 07/2014; 23(6):1460008

The simultaneous application of both link-blocking and path-integral factorization techniques is based on the observation that Monte Carlo updating of the three-dimensional smeared lattices preserves the key features of the long distance physics.

Thank you!